

Laplace expansions and tree decompositions: polytime algorithm for shallow nearest-neighbour Boson Sampling

Samo Novák^{1,2,3,4,*} and Raúl García-Patrón^{1,5,†}

¹Laboratory for the Foundations of Computer Science, School of Informatics, University of Edinburgh

²Mathematical Institute, University of Oxford

³ORCA Computing, London, UK

⁴Inria Paris, France

⁵Phasecraft Ltd., London, UK

(Dated: 24 December 2024)

In a Boson Sampling quantum optical experiment we send n individual photons into an m -mode interferometer and we measure the occupation pattern on the output. The statistics of this process depending on the permanent of a matrix representing the experiment, a #P-hard problem to compute, is the reason behind ideal and fully general Boson Sampling being hard to simulate on a classical computer. We exploit the fact that for a nearest-neighbour shallow circuit, i.e. depth $D = \mathcal{O}(\log m)$, one can adapt the algorithm by Clifford & Clifford [1] to exploit the sparsity of the shallow interferometer using an algorithm by Cifuentes & Parrilo [2] that can efficiently compute a permanent of a structured matrix from a tree decomposition. Our algorithm generates a sample from a shallow circuit in time $\mathcal{O}(n^2 2^\omega \omega^2) + \mathcal{O}(\omega n^3)$, where ω is the treewidth of the decomposition which satisfies $\omega \leq 2D$ for nearest-neighbour shallow circuits. The key difference in our work with respect to previous work using similar methods is the reuse of the structure of the tree decomposition, allowing us to adapt the Laplace expansion used by Clifford & Clifford which removes a significant factor of m from the running time, especially as $m > n^2$ is a requirement of the original Boson Sampling proposal.

I. INTRODUCTION

Boson Sampling was introduced by Aaronson & Arkhipov [3] in 2010 to propose a suitable candidate for the experimental demonstration of *quantum advantage*, which is when a quantum computer can efficiently solve a problem that a classical computer cannot [4]. Boson Sampling consists of sending n fully indistinguishable photons through an interferometer acting on m modes, and detecting the photons as they come out at the output of the interferometer. The work by Aaronson and Arkhipov provided strong evidence that such a quantum optics circuit would be hard to simulate on a classical computer when the interferometer was chosen at random from the Haar ensemble.

The intuition behind the hardness of Boson Sampling relies in the fact that its output probabilities require computing permanents of matrices that scale with the number of photons in the interferometer. The permanent of a matrix $A \in \mathbb{C}^{n \times n}$ is defined as

$$\text{per } A = \sum_{\sigma \in S_n} \prod_{i=1}^n A_{i,\sigma(i)},$$

where σ is a permutation from the symmetric group on n elements S_n . Despite its similarity with the definition of the determinant (without switching signs), computing the permanent exactly or approximating it for matrices


with complex entries is #P-hard [5]. The best known algorithms have exponential running time of $\mathcal{O}(n2^n)$: these are due to Ryser [6] and Glynn [7].

A celebrated theoretical result was the sampling algorithm by Clifford and Clifford that can generate an n -photon Boson Sampling output with a computational cost that is, up to a factor of 2, equivalent to the computation of the permanent of a matrix of size n . Specifically, the running time of their algorithm is $\mathcal{O}(n2^n) + \mathcal{O}(mn^2)$ [1].

The prospect of performing an experimental demonstration of quantum advantage attracted a lot of experimental effort and further theoretical work, which recently lead to experiments claiming they have reached quantum advantage on photonic platforms [8, 9]. It is known that one can design classical algorithms that exploit the presence of imperfections in the hardware, such as losses and distinguishability of photons, to run faster and potentially challenge the quantum advantage claims. For example, it was known that for integrated photonic circuits, composed on nearest-neighbour gates with transmission rates decaying exponentially with the depth of the circuit, circuits of depth $D = \Omega(\log m)$ may be simulated as thermal noise in polynomial time, and that a noisy shallow circuit can be simulated in quasi-polynomial time using tensor networks [10].

The fact that simulating a shallow circuit, i.e. with depth $D = \mathcal{O}(\log m)$, requires quasi-polynomial time was expected to be a feature of the use of tensor network techniques, rather than a fundamental result. It was believed that one could find a polynomial time algorithm, for example using results about efficient computation of permanents of sparse matrices by Cifuentes & Parrilo [2]. Indeed, this combination was used by Oh et al. in [11] to

*  0000-0002-2713-9593; samuel.novak@inria.fr

†  0000-0003-1760-433X; rgarcia3@exseed.ed.ac.uk

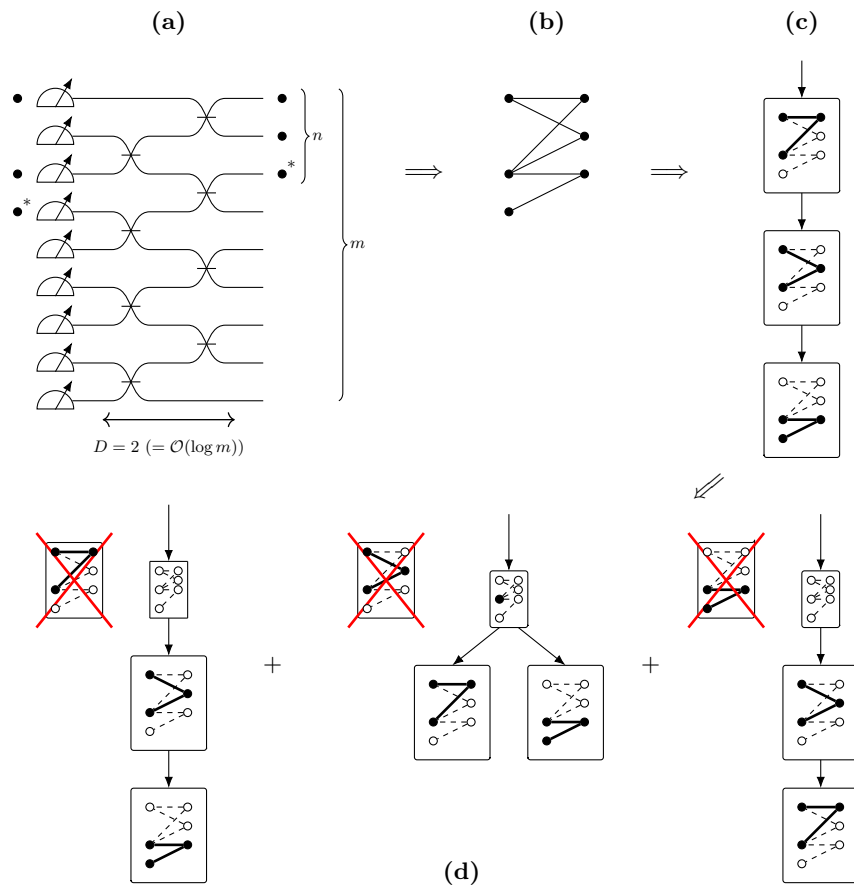


FIG. 1. An example overview of our enhancement to the algorithm of Clifford and Clifford by exploiting the tree decomposition algorithm by Cifuentes and Parrilo: **(a)** The shallow circuit of nearest-neighbour beamsplitters. We specify the positions of input photons, as well as the measurement outcome. The Cliffords’ algorithm builds a sample progressively by adding a new photon, shown here as “ \bullet^* ”, at the next unused input (RHS) and computing measurement probabilities of placing the corresponding \bullet^* at every possible output (LHS), conditioned on the previously sampled photons, shown here as “ \bullet ”. We show one of these outcomes. **(b)** We represent a given measurement outcome as a bipartite graph where vertices correspond to input (RHS), resp. output (LHS), photons of the Boson Sampling experiment. Edges are the nonzero transition amplitudes between these, and the sum of the weighted perfect matchings in this graph, i.e. the permanent, is the probability amplitude of the whole outcome of n photons. In our example, note the sparsity due to shallow depth of the interferometer. **(c)** To exploit the sparsity structure, we construct a tree decomposition: a tree structure where tree nodes contain sets of edges of the graph in (b), subject to simple rules. This structure is used by the Cifuentes and Parrilo algorithm, filling a set of tables using a dynamical programming algorithm to efficiently compute the permanent. We use a tree decomposition where the underlying tree is linear (no branching) and each node corresponds uniquely to an input photon vertex. **(d)** The implementation of the Laplace expansion using our tree decomposition. Each summand corresponds to removing a different input photon vertex. This is done in sequence and can be understood as a “machine head” walking the tree from one end to the other (in analogy to a Turing machine head walking a tape). At each step, corresponding to a summand in the Laplace expansion, the head moves to the next tree node, makes this the root by orienting the rest of the tree away, and temporarily replaces it by an (almost) empty node, as shown in the picture. This corresponds to taking a submatrix by removing the column associated to the temporarily replaced node. At each such step, the Cifuentes and Parrilo dynamical programming algorithm computes the permanent of the submatrix from this modified tree. We then use these permanents in the Laplace expansion to compute the marginal probability amplitude of a given new output mode where the photon \bullet^* is measured. We repeat this procedure for all possible choices of the new output mode.

prove some complexity results about the (non)-hardness of Boson Sampling circuits with a lattice structure. Furthermore, an efficient algorithm for shallow Gaussian Boson Sampling circuits, a variant of Boson Sampling using squeezed states instead of single photons, was proven by Qi et al. in [12] using similar ideas.

In this work we revisit the initial conjecture in [10]

and show how one can use the result of Cifuentes and Parrilo [2] to design a polynomial time algorithm for Boson Sampling from shallow circuits, exploiting the fact that the computation of a permanent scales polynomially in the treewidth of the graph corresponding to our photonic circuit of interest. A similar approach was given by Oh et al. [11] who gave the running time of $\mathcal{O}(mn^2 2^{\omega\omega^2})$.

We present an algorithm that reproduces all the key advantages of the initial Clifford and Clifford algorithm in [1] adapted to the nearest-neighbors shallow circuit scenario. Our main technical contribution is the following: We adapt the use of sparsity of matrices in the algorithm by Cifuentes and Parillo [2] to combine it with the use of the Laplace expansion in the algorithm by Clifford and Clifford. We do this in a time-efficient manner to remove the dependency on the number of modes in [11], achieving a running time of $\mathcal{O}(n^{22\omega\omega^2}) + \mathcal{O}(\omega n^3)$.

A. Informal summary

Here, and in the running example of Figure 1, we give an informal summary of the present work. A measurement outcome of a Boson Sampling experiment, defined by giving the interferometer and input and output states (see Fig. 1a) can be represented by a bipartite graph encoding the connectivity of the interferometer (see Fig. 1b). Here, the vertices in the two partitions correspond to input, resp. output photons, and weighted edges correspond to nonzero transition amplitudes between individual photon positions. The probability amplitude of measuring the whole outcome of several indistinguishable photons is the sum over the perfect matchings in this graph, i.e. the permanent. In the shallow regime, the graph in Fig. 1b is sparse, and we capture this sparsity using a *tree decomposition* in Fig. 1c, where we group edges of the graph into nodes of a new tree structure, subject to simple connectivity conditions. The algorithm of Cifuentes and Parrilo exploits this tree decomposition to compute the permanent efficiently using a dynamical program [2].

Our main technical contribution is shown in Figure 1d of the running example. We adapt the use of the Laplace expansion of the permanent, a vital component of the algorithm by Clifford and Clifford [1], to the permanent computation using tree decompositions. Computing the probability of the k -th photon at a given output r_k , given a pattern of input and output modes for the previous $k-1$ photons is captured by the permanent $\text{per } \mathcal{W}^{(r_k)}$ of a matrix where only the last row depends on the choice of the new possible photon output r_k . Clifford and Clifford [1] use the Laplace expansion:

$$\text{per } \mathcal{W}^{(r_k)} = \sum_{j=1}^k \mathcal{W}_{k,j}^{(r_k)} \text{per } \mathcal{W}_{\diamond(k,j)}^{(r_k)}. \quad (1)$$

where $\mathcal{W}_{\diamond(k,j)}^{(r_k)}$ is the submatrix of $\mathcal{W}^{(r_k)}$ with row k and column j removed. As we remove the last row k , these matrices are independent of the choice of r_k . Clifford and Clifford exploit this fact to precompute the values of $\{\text{per } \mathcal{W}_{\diamond(k,j)}^{(r_k)}\}_j$ to later separately do a simple calculation of the m possible output probabilities in polynomial time.

A naive approach to adapt the Cifuentes and Parrilo algorithm for nearest-neighbor shallow circuits would require a new tree decomposition for each of these submatrices, which degrades performance. However, by ensuring

that the nodes of the tree decomposition we use are in 1-to-1 correspondence to input photon vertices, and that the tree is linear (no branching, i.e. isomorphic to a path graph), we can compute each summand in the Laplace expansion by only a small modification of the original tree decomposition. Concretely, one can imagine a “machine head” walking the tree from one end to the other (in analogy to the head of a Turing machine walking the tape), and temporarily replacing it to delete the corresponding column of the matrix (the j in $\mathcal{W}_{\diamond(k,j)}^{(r_k)}$ above). After computing $\text{per } \mathcal{W}_{\diamond(k,j)}^{(r_k)}$ from this modified tree, it then returns the original node, and moves to the next one. In Fig. 1d, we show the three summands and the replacement of nodes that implements the Laplace expansion for our running example.

B. Structure of the paper

The following three sections introduce the material needed to understand our result: In Section II, we introduce the basic concepts of Boson Sampling and quantum optics needed for our work. In Section III, we give a pedagogical introduction to the Clifford and Clifford algorithms for simulating Boson Sampling classically. Then in Section IV, we introduce the tree decomposition of matrices and the algorithm of Cifuentes and Parillo for computing permanents of sparse matrices.

Before we can adapt these algorithms together, in Section V, we introduce a few basic definitions of photonic circuits, as well as observe some basic results about tree decomposition needed for our main result. Finally, in Section VI, we present our new algorithm, and we conclude and discuss open problems in Section VII.

To facilitate reading, we omit some simple but lengthy derivations and proofs in the main body, and we present them instead in the Appendix.

II. BOSON SAMPLING

In an ideal Boson Sampling circuit, the input and output can be written in a basis of quantum states corresponding to the location of n photons in m modes. These are represented as *number (Fock) states* $|\underline{n}\rangle = |n_1, \dots, n_m\rangle \in (\mathbb{C}^n)^{\otimes m}$, where $n_i \in \mathbb{N}$ is the number of photons in mode i , and $\sum_i n_i = n$. These states are canonically written using the creation operators as

$$|\underline{n}\rangle = \prod_{i=1}^m \frac{(\hat{a}_i^\dagger)^{n_i}}{\sqrt{n_i!}} |0\rangle^{\otimes m},$$

where \hat{a}_i^\dagger acts only on mode i . An *interferometer* is a linear optical device that is represented by a unitary matrix $\mathcal{U} \in \mathbb{U}(m)$ acting linearly on the m creation operators as

$$\hat{a}_i^\dagger \xrightarrow{\mathcal{U}} \sum_{j=1}^m \mathcal{U}_{i,j} \hat{a}_j^\dagger \quad \forall i = 1, \dots, m. \quad (2)$$

The unitarity of U (i.e. $U^\dagger U = U U^\dagger = \mathbb{1}$) ensures the total number of photons is preserved [13].

A. First quantization representation

It is sometimes useful to represent these states using first quantization representation, where every photon corresponds to a *qudit* of dimension m . Its logical information encodes the mode in which the photon is located. We ensure the indistinguishability of photonic states by writing the global quantum state as a symmetric superposition over all permutations of the qudits. The qudit representation was used in [14] to design a qubit-based simulation of boson sampling.

For a given occupation state $|\underline{n}\rangle$, we start by writing an n -qudit state where each qudit represents a photon in a specified mode, and these are arranged in a non-decreasing order:

$$|\underline{z}\rangle := |1\rangle^{\otimes n_1} \otimes |2\rangle^{\otimes n_2} \otimes \dots \otimes |m\rangle^{\otimes n_m}. \quad (3)$$

Any permutation σ of the n qudits will provide a new basis state $|\underline{r}\rangle = \sigma|\underline{z}\rangle$ that has the same mode occupation pattern as $|\underline{z}\rangle$, given by $|\underline{n}\rangle$. The states corresponding to the same number state are considered equivalent, written $|\underline{z}\rangle \sim |\underline{r}\rangle$. The size of each equivalence class of states $|\underline{r}\rangle$ with the same mode distribution as $|\underline{z}\rangle$ is given by

$$\binom{n}{n_1, \dots, n_m} = \frac{n!}{\prod_{i=1}^m n_i!}. \quad (4)$$

In the notation of $|\underline{z}\rangle$ and $|\underline{r}\rangle$, the qudits are assigned specific locations and are therefore distinguishable. To ensure indistinguishability, the state $|\Phi_{\underline{n}}\rangle$ corresponds to the symmetric superposition of all their permutations:

$$|\Phi_{\underline{n}}\rangle = \frac{1}{\sqrt{n! \cdot \prod_{i=1}^m n_i!}} \sum_{\sigma \in S_n} \sigma|\underline{z}\rangle, \quad (5)$$

where σ is a permutation in the symmetric group on n elements S_n , and the prefactor on the RHS is its normalization [14].

The action of the interferometer \mathcal{U} in the first-quantization representation follows from (2). For a single qudit $|i\rangle$, the action reads:

$$|i\rangle \xrightarrow{\mathcal{U}} \sum_{j=1}^m \mathcal{U}_{i,j} |j\rangle = \mathcal{U} |i\rangle, \quad (6)$$

which results from its action on \hat{a}_i^\dagger and the fact that $|i\rangle = \hat{a}_i|0\rangle$. Likewise, product states correspond to products of creation operators, which give the relation

$$|\underline{z}\rangle \equiv \bigotimes_{k=1}^n |z_k\rangle \mapsto \bigotimes_{k=1}^n (\mathcal{U} |z_k\rangle) = \mathcal{U}^{\otimes n} |\underline{z}\rangle, \quad (7)$$

where we have introduced the notation $|z_i\rangle$ to mean the i -th qudit in the product (3). By linearity we obtain that $|\Phi_{\underline{n}}\rangle \mapsto \mathcal{U}^{\otimes n} |\Phi_{\underline{n}}\rangle$, i.e. in the first quantization representation, the linear optical circuit unitary over n photons acts as $\mathcal{U}^{\otimes n}$.

B. Boson Sampling outcome probabilities

For a given input state $|\underline{n}\rangle$ the output probability distribution of a boson sampling circuit of interferometer \mathcal{U} is given by the Born rule:

$$\mathbb{P}[\underline{n}'|\underline{n}] = |\langle \Phi_{\underline{n}'} | \mathcal{U}^{\otimes n} | \Phi_{\underline{n}} \rangle|^2 \quad (8)$$

where $|\underline{n}'\rangle$ is the output of the photon number measurement, and where we have $\sum_i n'_i = \sum_i n_i = n$, as the photon number is preserved by ideal lossless circuits. For completeness, in Appendix A1 we rewrite the derivation in [14] of the permanent rule using the first quantization representation. In a nutshell, using the definition in equation (5) and action in (7), one can show

$$\mathbb{P}[\underline{n}'|\underline{n}] = \left| \frac{1}{\sqrt{\prod_{i=1}^m n_i! n'_i!}} \sum_{\pi \in S_n} \prod_{j=1}^n \langle z'_j | \mathcal{U} | z_{\pi(j)} \rangle \right|^2 \quad (9)$$

where z_i is the mode of the i -th input photon, and z'_j is the mode of the j -th output photon. By introducing a compact notation

$$\mathcal{V}_{l,h}^{\underline{n}',\underline{n}} := \langle z'_l | \mathcal{U} | z_h \rangle, \quad (10)$$

for the matrix elements of \mathcal{U} at row (output) z'_l and column (input) z_h , we obtain the simplification

$$\mathbb{P}[\underline{n}'|\underline{n}] = \left| \frac{1}{\sqrt{\prod_{i=1}^m n_i! n'_i!}} \sum_{\pi \in S_n} \prod_{j=1}^n \mathcal{V}_{j,\pi(j)}^{\underline{n}',\underline{n}} \right|^2 \quad (11)$$

where we recognize the definition of the permanent, leading to the final result

$$\mathbb{P}[\underline{n}'|\underline{n}] = \frac{|\text{per } \mathcal{V}^{\underline{n}',\underline{n}}|^2}{\prod_{i=1}^m n_i! \cdot n'_i!}. \quad (12)$$

1. Construction of $\mathcal{V}^{\underline{n}',\underline{n}}$

While $\mathcal{U} \in \mathbb{C}^{m \times m}$ represents an operator acting on modes, the matrix $\mathcal{V}^{\underline{n}',\underline{n}} \in \mathbb{C}^{n \times n}$ encodes the behaviour of the n photons as they pass through the interferometer. In general, we get $\mathcal{V}^{\underline{n}',\underline{n}} \in \mathbb{C}^{n \times n}$ by taking n'_i copies of row i in \mathcal{U} , creating an $n \times m$ matrix, and from this n_j copies of column j [14]. In particular, note that if the input (resp. output) photons do not occupy some mode j , the corresponding column (row) j of \mathcal{U} will not be part of $\mathcal{V}^{\underline{n}',\underline{n}}$. Similarly, if k photons are in the same input (output) mode, then the corresponding column (row) will have k repetitions.

Example II.1. For $n = n' = 3$, $m = 5$, let the input be $|\underline{n}\rangle = |1, 1, 1, 0, 0\rangle$, corresponding to $|\Phi_{\underline{n}}\rangle = \frac{1}{\sqrt{6}} \sum_{\sigma \in S_3} \sigma |1\rangle|2\rangle|3\rangle$, and output $|\underline{n}'\rangle = |2, 0, 0, 1, 0\rangle$, corresponding to $|\Phi_{\underline{n}'}\rangle = \frac{1}{\sqrt{12}} \sum_{\sigma \in S_3} \sigma |1\rangle|1\rangle|4\rangle$. Then we

have for example $\mathcal{V}_{1,1}^{\underline{n}',\underline{n}} = \langle z'_1 | \mathcal{U} | z_1 \rangle = \langle 1 | \mathcal{U} | 1 \rangle = \mathcal{U}_{1,1}$ and $\mathcal{V}_{2,3}^{\underline{n}',\underline{n}} = \langle z'_2 | \mathcal{U} | z_3 \rangle = \langle 1 | \mathcal{U} | 3 \rangle = \mathcal{U}_{1,3}$. The full matrix reads:

$$\mathcal{V}^{\underline{n}',\underline{n}} = \begin{pmatrix} \mathcal{U}_{1,1} & \mathcal{U}_{1,2} & \mathcal{U}_{1,3} \\ \mathcal{U}_{1,1} & \mathcal{U}_{1,2} & \mathcal{U}_{1,3} \\ \mathcal{U}_{4,1} & \mathcal{U}_{4,2} & \mathcal{U}_{4,3} \end{pmatrix}.$$

Observe that the columns in $\mathcal{V}^{\underline{n}',\underline{n}}$ come from columns 1, 2 and 3 of \mathcal{U} , resulting from the occupation number of the input. Similarly, we see that rows 1 and 2 of $\mathcal{V}^{\underline{n}',\underline{n}}$ are the same, which corresponds to mode 1 being occupied by two photons at the output. The last row contains elements from the fourth row of \mathcal{U} , because one of the output photons occupies mode 4.

2. Graphical representation

In Sections V and VI, we will make use of the following graphical representation of matrices \mathcal{U} and $\mathcal{V}^{\underline{n}',\underline{n}}$ using bipartite graphs $G(\mathcal{U})$ and $G(\mathcal{V}^{\underline{n}',\underline{n}})$, as shown in Figure 2. Each matrix is understood as a linear combination of outer products in the standard basis, and these become the edges of the corresponding graph, weighted by the matrix elements.

The bipartite graph $G(\mathcal{U})$ encodes the input-output relation of the linear interferometer. Every vertex corresponds to either an input or output mode, and edges are weighted by the amplitude of the given input-output transition. The graph $G(\mathcal{V}^{\underline{n}',\underline{n}})$ represents the possible *paths* that all the photons may take from input $|\underline{z}\rangle$ to output $|\underline{z}'\rangle$. The vertices on the right (columns of $\mathcal{V}^{\underline{n}',\underline{n}}$) are the input positions (modes), and on the left are output positions. Note that an output mode i may repeat, in which case there are multiple copies, labeled $|i\rangle_1, |i\rangle_2, \dots$

Each photon starts and ends at a single vertex of $G(\mathcal{V}^{\underline{n}',\underline{n}})$, different from the other photons. This corresponds to a perfect matching on $G(\mathcal{V}^{\underline{n}',\underline{n}})$. Photons are indistinguishable, which means that any perfect matching corresponds to a possible way that the input $|\underline{z}\rangle$ was transformed into the output $|\underline{z}'\rangle$. Then the probability amplitude of transition from $|\underline{n}\rangle$ to $|\underline{n}'\rangle$ is the sum of the weights of all perfect matchings, where a weight of a matching is the product of the weights of its edges. Indeed, the sum of the perfect matching weights is the permanent per $\mathcal{V}^{\underline{n}',\underline{n}}$, and we show this interpretation of the permanent in the simple example of Fig. 3. Furthermore, note that one can understand this as a Feynman-style sum over histories, where each perfect matching represents the paths taken by the photons.

C. Probability in qudit representation

In the first quantization (qudit) representation of Boson Sampling, counting the photon number per mode can be implemented with the Schur transform circuit W

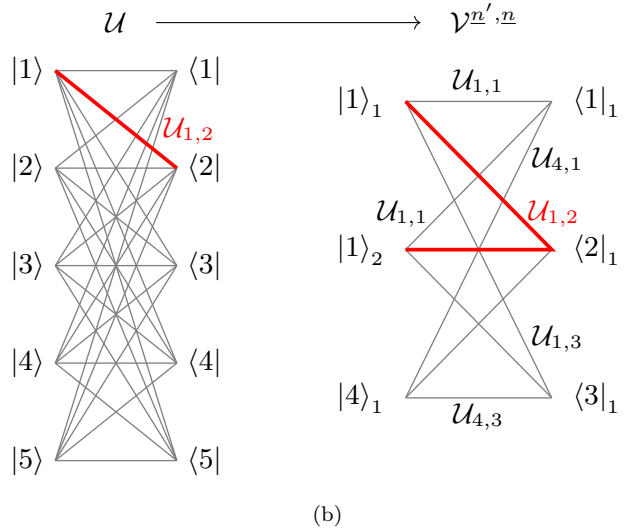
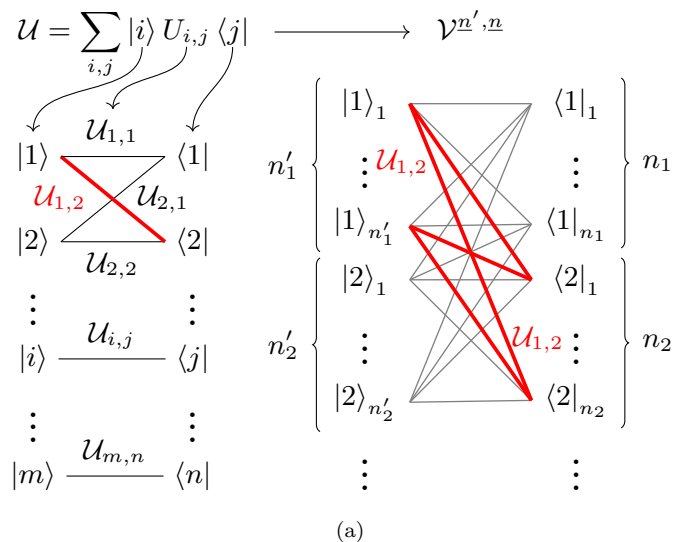


FIG. 2. Bipartite **graphical representation**. (a) Graphs $G(\mathcal{U})$ and $G(\mathcal{V}^{\underline{n}',\underline{n}})$ of matrices \mathcal{U} and $\mathcal{V}^{\underline{n}',\underline{n}}$, respectively, and their relationship. Vertices on the left are outputs, while the inputs are on the right. Note that \mathcal{U} is the adjacency matrix of $G(\mathcal{U})$, and likewise $\mathcal{V}^{\underline{n}',\underline{n}}$ is the adjacency matrix of $G(\mathcal{V}^{\underline{n}',\underline{n}})$. The output (left) partition of the graph $G(\mathcal{V}^{\underline{n}',\underline{n}})$ is obtained by taking n'_i copies of output vertex $|i\rangle$ of $G(\mathcal{U})$ – these copies are labelled $|i\rangle_a$ for $a = 1, \dots, n'_i$. Similarly, the input (right) partition gets n_j copies of input $\langle j|$ from $G(\mathcal{U})$. If there is an edge $e = (|i\rangle, \langle j|)$ in $G(\mathcal{U})$, then $G(\mathcal{V}^{\underline{n}',\underline{n}})$ has edges $(|i\rangle_a, \langle j|_b)$ for all a, b , and these have the same weight as e . We emphasize the edge $(|1\rangle, \langle 2|)$ of $G(\mathcal{U})$ and its copies in $G(\mathcal{V}^{\underline{n}',\underline{n}})$, all with weights $\mathcal{U}_{1,2}$. Some edges, particularly in $G(\mathcal{U})$, are omitted for clarity. (b) Graphical representation of Example II.1.

followed by a measurement of the photon number per mode [14]. Interestingly, this measurement is equivalent to directly measuring the qudits before the Schur transform, i.e. measuring the qudit occupation basis $|\underline{z}\rangle$ and later mapping the result to the mode occupation basis $|\underline{n}\rangle$. The latter step is done by forgetting the individual

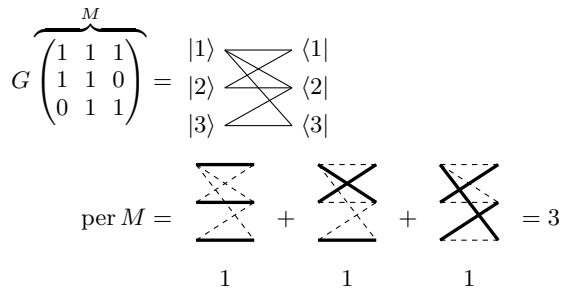


FIG. 3. Connection between permanents and graphs of matrices. In this example, when the matrix is just an adjacency matrix, i.e. the weights of existing edges are all 1, the permanent counts the number of perfect matchings. In general, edges would have different weights, and for each matching, its value is the product of the weights of its chosen edges.

information of each qudit and storing only the number of photons per mode. The validity of this statement result from the relation:

$$\mathbb{P}[\underline{z}'|\underline{n}] = |\langle \underline{z}' | \mathcal{U}^{\otimes n} | \Phi_{\underline{n}} \rangle|^2 = \frac{\prod_{i=1}^m n'_i!}{n!} |\langle \Phi_{\underline{n}'} | \mathcal{U}^{\otimes n} | \Phi_{\underline{n}} \rangle|^2,$$

where the last equality results from the invariance of $\mathcal{U}^{\otimes n}$ w.r.t. permutations and the definition of $|\Phi_{\underline{n}}\rangle$ in (5). This leads to the relation

$$\mathbb{P}[\underline{n}'|\underline{n}] = \frac{n!}{\prod_{i=1}^m n'_i!} \mathbb{P}[\underline{z}'|\underline{n}]. \quad (13)$$

Sampling in the $|\underline{z}\rangle$ basis followed by the mapping to $|\underline{n}\rangle$ is a central concept in the algorithm of Clifford and Clifford which we summarize in Section III.

III. CLIFFORD AND CLIFFORD ALGORITHMS

The work [1] by Clifford and Clifford presents two algorithms: the first has running time that scales as $\mathcal{O}(mn3^n)$. The second takes $\mathcal{O}(n2^n)$ steps, where not only the exponent is improved, but the dependency on m is removed from the costly exponential term, and transferred to a less significant polytime term. For pedagogical reasons we revisit their work in three steps, presenting one new tool at a time and discussing its running time.

A. Variable origins of photons and algorithm CC-A

The idea behind Algorithm A in Clifford and Clifford [1] (referred to as CC-A) consists of sampling in the $|\underline{r}\rangle$ basis (see Section II A) using a standard chain rule procedure. This can be understood as follows: We work as if the photons were distinguishable by assigning them a specific output locations, but later restoring their indistinguishability by properly engineering the conditional probabilities,

as shown below, and finally post-processing the output \underline{r} to \underline{n} by counting the occupancy of modes. The chain rule states that

$$p(r_1, \dots, r_n) = p(r_1)p(r_2|r_1) \cdots p(r_n|r_{n-1}, \dots, r_1). \quad (14)$$

If one has access to all marginals of $p(r_1, r_2, \dots, r_n)$, one can generate a sample using the chain rule by first computing $p(r_1)$ for all $r_1 = 1, \dots, m$, and committing to a choice of r_1 following the computed probability distribution. Having fixed r_1 , we compute $p(r_1, r_2)$ for all $r_2 = 1, \dots, m$, using $p(r_2|r_1) = p(r_1, r_2)/p(r_1)$, and again commit to a choice of r_2 following that distribution. Here, we use the value $p(r_1)$ computed in the previous step. Iterating this procedure, we can generate one sample via the computation of mn marginals. In [1], it was shown that the marginals read

$$p(r_1, \dots, r_k) = \frac{(n-k)!}{n!} \sum_{\substack{C \subseteq [n] \\ |C|=k}} \left| \text{per } \tilde{\mathcal{V}}^{(r_1, \dots, r_k), C} \right|^2, \quad (15)$$

for which we give a complete derivation in Appendix A 1. Recall the notation $[n] = \{1, \dots, n\}$. In a partial sample of k photons, we need to sum over all possible choices of photons from the input state $|\underline{n}\rangle = |1^n, 0^{m-n}\rangle$ which may have ended up in the specified outputs (r_1, \dots, r_k) . These are represented by the sets C , and there are $\binom{n}{k}$ possible choices. These sets select the columns of \mathcal{U} , hence the notation C .

The matrix $\tilde{\mathcal{V}}^{(r_1, \dots, r_k), C}$ fulfils the same function as $\mathcal{V}^{\underline{n}', \underline{n}}$; the difference is that the latter is given by specifying number states, while the former is given in the qudit representation, i.e. giving photon locations:

$$\tilde{\mathcal{V}}_{i,j}^{(r_1, \dots, r_k), C} = \langle r_i | \mathcal{U} | c_j \rangle,$$

where the input qudits are given as an (unordered) set $C = \{c_1, \dots, c_k\}$, so we impose $c_1 \leq c_2 \leq \dots \leq c_k$ for convenience. We can choose any ordering here, because the permanent is invariant under permutations of columns, as well as rows. Note that only the presence or absence of a row or column is relevant (or, more generally, its number of repetitions), but we choose an ordering so that we can write down concrete matrices. Note further that we always give the output photons (r_1, \dots, r_k) in the order in which they are sampled. The latter ensures that the newest photon, for which we are computing the marginal probability, corresponds to the last row of the matrix, and this convention is useful to conveniently formulate the Laplace expansion in Section III C, as well as our enhancements in Section VI.

1. Running time

The algorithm CC-A samples from $p(r_1, \dots, r_n)$ by committing to the partial sample (r_1, \dots, r_{k-1}) and extending it by a single r_k at each step $k = 2, \dots, n$. For every k

we need to compute m marginals, each consisting of a sum of size $\binom{n}{k}$ and a permanent of a matrix of size $k \times k$ taking the time $\mathcal{O}(k2^k)$ steps each using the algorithm by Ryser [6] or Glynn [7]. This leads to a total running time:

$$\mathcal{O}\left(m \sum_{k=1}^n k2^k \binom{n}{k}\right) = \mathcal{O}(mn3^n). \quad (16)$$

At each step k , we need to remember the values $\{p(r_k|r_1, \dots, r_{k-1})\}_{r_k=1, \dots, m}$, i.e. store a vector of m values. Therefore we require $\mathcal{O}(m)$ additional memory, less than the memory needed to store the matrix \mathcal{U} of size $\mathcal{O}(m^2)$.

B. Removing the costly sum: algorithm CC-B

The first improvement of CC-A suggested by Clifford and Clifford [1], which we refer to as CC-B, is to remove the costly sum over $\binom{n}{k}$ terms corresponding to sets C by randomly preselecting one of them, and only using the inputs (columns) in the chosen C . To do this, choose a uniformly permutation $\alpha \in S_n$ and use it to permute the input photons, i.e. permute the columns of \mathcal{U} . Remark that one needs to generate a new permutation for each new generated sample. As shown in [1], and reproduced in Appendix B2 for completeness, the expectation value over many samples, each with a uniformly random α , leads to the correct marginal probability:

$$p(r_1, \dots, r_k) = \mathbb{E}_{\alpha \in S_n} \left[\frac{1}{k!} \left| \text{per } \tilde{\mathcal{V}}^{(r_1, \dots, r_k), \alpha([k])} \right|^2 \right], \quad (17)$$

where $\alpha([k]) = \{\alpha(i) \mid i \in [k]\}$. For each photon k , the $1/k!$ is a shared constant prefactor present in (17) for each value of r_k . Similarly to CC [1], for convenience, we can omit this shared prefactor in the algorithm and sample from unnormalized pmfs. This is possible using the Walker's alias method in time $\mathcal{O}(m)$ for a pmf stored in an array of length m , the latter being the number of possible new modes [15].¹

1. Running time

The running time of Algorithm CC-B scales as

$$\mathcal{O}\left(m \sum_{k=1}^n k2^k\right) = \mathcal{O}\left(mn \sum_{k=1}^n 2^k\right) = \mathcal{O}(mn2^{n+1}). \quad (18)$$

Hence CC-B generates a sample in time $\mathcal{O}(mn2^n)$. Similarly to CC-A, it requires additional space $\mathcal{O}(m)$, where m is the number of modes.

C. Laplace expansion: algorithm CC-C

The final improvement of [1] allows to transfer the prefactor m from the dominant exponential term to a less relevant quadratic term, leading to an algorithm that generates a sample with a factor of 2 of the cost of computing a single output probability. This result is achieved by a clever use of the Laplace expansion of the permanent, defined below.

The central idea exploits the fact that when expanding the sample from $k-1$ to k photons, we need to compute m permanents where all k columns of $\tilde{\mathcal{V}}^{(r_1, \dots, r_k), \alpha([k])}$ are shared, and all rows except one are also the same. The rows r_1, \dots, r_{k-1} (corresponding to previously sampled output photons) and columns $\alpha([k]) = \{\alpha(1), \dots, \alpha(k)\}$ (predetermined input photons) are fixed, so we simplify notation as follows: Denote $\mathcal{W} = \tilde{\mathcal{V}}^{(r_1, \dots, r_{k-1}), \alpha([k])}$ the $(k-1) \times k$ matrix containing the shared rows and columns, and denote $\mathcal{W}^{(r_k)} = \tilde{\mathcal{V}}^{(r_1, \dots, r_k), \alpha([k])}$, i.e. adding the row r_k of \mathcal{U} to \mathcal{W} , for each choice of a new photon mode $r_k \in [m]$. Using the Laplace expansion of the permanent, we write:

$$\text{per } \mathcal{W}^{(r_k)} = \sum_{j=1}^k \mathcal{W}_{k,j}^{(r_k)} \text{per } \mathcal{W}_{\diamond(k,j)}^{(r_k)} \quad (19a)$$

$$= \sum_{j=1}^k \mathcal{U}_{r_k, \alpha(j)} \text{per } \mathcal{W}_{\diamond j}. \quad (19b)$$

In Eq. (19a), $\mathcal{W}_{\diamond(k,j)}^{(r_k)}$ is the $(k-1) \times (k-1)$ submatrix of $\mathcal{W}^{(r_k)}$ with the row k and column j removed. By construction, the matrices $\mathcal{W}_{\diamond(k,j)}^{(r_k)}$ are the same for all choices of r_k , because all rows except r_k are fixed. In Eq. (19b), we replace this by $\mathcal{W}_{\diamond j}$ denoting the $(k-1) \times (k-1)$ submatrix of \mathcal{W} , the matrix with shared rows and columns, with column j removed.

The final improvement by Clifford and Clifford is an adaptation of the Glynn's permanent algorithm [7] to compute the family of the permanents $\{\text{per } \mathcal{W}_{\diamond j}\}_{j=1}^k$ in combined time $\mathcal{O}(k2^k)$ and space $\mathcal{O}(k)$. This is the same scaling, up to a constant, as that required to compute the permanent of the whole $k \times k$ matrix using Glynn's formula, with summation ordered using the Gray code (see [1, proof of Lemma 2]). Once these permanents are known, computing the m output probabilities requires only the use of the Laplace expansion (19b). This last step requires $\mathcal{O}(mk)$ operations.

We refer to this algorithm as CC-C and provide the pseudo-code in Figure 4. In Sections V and VI, we adapt this idea to the tree decomposition method developed by Cifuentes and Parrilo to obtain a polynomial-time algorithm to sample from shallow circuits.

¹ Precisely, the time per sample is $\mathcal{O}(1)$ after pre-processing time of $\mathcal{O}(m)$. In our use case, we need a single sample from each pmf, so we characterize the time as just the total $\mathcal{O}(m)$.

Algorithm CC-C: Boson Sampling

Input:

- the number of modes m , and the number of photons n , both positive integers, s.t. $n \leq m$
- matrix $U \in \mathbb{U}(m)$, a Haar random unitary representing an interferometer

Result: a single sample z'

```

1  $\alpha \leftarrow$  uniformly random permutation from  $S_n$ 
2  $\mathcal{V}^{\mathbb{Z}}$   $\leftarrow$  first  $n$  columns of  $U$  permuted using  $\alpha$ 
3 initialize  $\underline{r} = (r_1, \dots, r_n) \leftarrow (0, \dots, 0)$ 
  /* first photon (permanents are just matrix
  elements) */
4 compute  $w_1(i) \leftarrow |\mathcal{V}_{i,1}^{\mathbb{Z}}|^2$  for  $i \in [m]$ 
5  $r_1 \leftarrow$  sample from the pmf  $w_1$ 
  /* rest of the sample */
6 for  $k \leftarrow 1, \dots, n-1$  do
7    $\mathcal{W} \leftarrow$  rows  $r_1, \dots, r_k$  and first  $k+1$  columns of  $\mathcal{V}^{\mathbb{Z}}$ 
   (corresponding to  $\tilde{\mathcal{V}}^{(r_1, \dots, r_k), \alpha([k+1])}$ )
8   compute  $\{\text{per } \mathcal{W}_{\circ i}\}_{i=1}^{k+1}$ 
9   compute  $w_{k+1}(i) \leftarrow \left| \sum_{j=1}^{k+1} \mathcal{V}_{i,j}^{\mathbb{Z}} \text{per } \mathcal{W}_{\circ j} \right|^2$  for
    $i \in [m]$ 
10   $r_{k+1} \leftarrow$  sample from the (unnormalised) pmf  $w_{k+1}$ 
11  $\underline{z}' \leftarrow$  sort  $\underline{r}$  in non-decreasing order
12 return  $\underline{z}'$ , which represents  $|\Phi_{\underline{z}'}\rangle = \frac{1}{(\dots)} \sum_{\sigma \in S_n} \sigma |z'\rangle$ 

```

FIG. 4. Pseudocode of algorithm CC-C for classically simulating Boson Sampling.

1. Running time

The running time of CC-C is:

$$\sum_{k=1}^n \left(\mathcal{O}(k2^k) + \mathcal{O}(mk) \right) = \mathcal{O} \left(n \sum_{k=1}^n 2^k \right) + \mathcal{O} \left(m \sum_{k=1}^n k \right) \quad (20a)$$

$$= \mathcal{O}(n2^{n+1}) + \mathcal{O}(mn^2). \quad (20b)$$

In (20a), we use the fact that $k \leq n$ to bound $k2^k = \mathcal{O}(n2^n)$. The summation $\sum_{k=1}^n 2^k = 2(2^n - 1)$, and together these give the term $n2^{n+1}$ in (20b). Algorithm CC-C generates a sample in time $\mathcal{O}(n2^n) + \mathcal{O}(mn^2)$, requiring space $\mathcal{O}(m)$. To our knowledge, CC-C is currently the best algorithm to simulate Boson Sampling in the regime with no collisions and no additional constraints, e.g. on the depth of the circuit.

IV. CIFUENTES AND PARRILO ALGORITHM

In this section we present the concept of *tree decompositions* of a graph and its use in the algorithm by Cifuentes and Parrilo (CP) to compute the permanent of sparse matrices using dynamic programming [2].

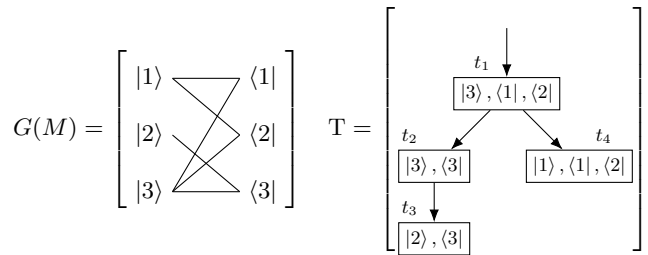


FIG. 5. Example of a tree decomposition $T = (T, \rho, \kappa)$ of $G(M)$, the graph of matrix $M = \begin{pmatrix} \bullet & \bullet & 0 \\ 0 & 0 & \bullet \\ \bullet & \bullet & \bullet \end{pmatrix}$, where the \bullet implies a nonzero element. This tree is rooted at t_1 .

A. Tree Decompositions

A tree decomposition is a structure that captures how connected or disconnected a graph is, and it can under some conditions speed up the computation of solutions of instances of problems that are otherwise worst-case NP-hard [16]. Finding an optimal tree decomposition can itself be NP-hard, however, there exist good heuristics that allow improvements for practical problems. An example where tree decomposition is used by the quantum information community is the optimization of tensor network contractions. In our case, the Cifuentes and Parrilo algorithm exploits tree decompositions to compute permanents of structured matrices faster than using the standard algorithms by Ryser or Glynn.

In this work we are interested in a *bipartite* graph G where the set of vertices V consists of rows \mathcal{R} and columns \mathcal{C} , and the edges, each connecting one row and one column, correspond to the matrix elements, as shown in Figure 5. The sets \mathcal{R} and \mathcal{C} are disjoint, i.e. $V = \mathcal{R} \sqcup \mathcal{C}$.

In the following, we use the notation 2^X for the powerset of a set X , that is the set of all subsets of X .

Definition IV.1 (tree decomposition of a bipartite graph). Let $G = (V = \mathcal{R} \sqcup \mathcal{C}, E \subseteq \mathcal{R} \times \mathcal{C})$ be a bipartite graph. A tree decomposition $T = (T, \rho, \kappa)$ is a triple consisting of a tree T rooted in $\text{root}(T)$, where for each node $t \in T$, we denote $\text{ch}(t)$ the unordered set of its children; and the functions $\rho : T \rightarrow 2^{\mathcal{R}}$ and $\kappa : T \rightarrow 2^{\mathcal{C}}$ that label the nodes with subsets of \mathcal{R} and \mathcal{C} . We say that a node $t \in T$ *contains* the elements of $\rho(t)$ and $\kappa(t)$. A tree decomposition must satisfy the following axioms:

- (T1) The union of contents over the entire tree covers all vertices of the graph: $\rho(T) = \mathcal{R}$ and $\kappa(T) = \mathcal{C}$, where we denote $\rho(T) = \bigcup_{t \in T} \rho(t)$, and analogously $\kappa(T) = \bigcup_{t \in T} \kappa(t)$.
- (T2) Every edge of the graph is contained in some node of the tree. This means that for each $(r, c) \in E$, there exists a node $t \in T$ that contains both its endpoints, i.e. $r \in \rho(t)$ and $c \in \kappa(t)$.
- (T3) For every $r \in \mathcal{R}$ (resp. $c \in \mathcal{C}$), the set of all nodes that contain it is a subtree of T , i.e. all nodes

containing r (resp. c) are connected in T .²

By convention, we write the decomposition upright as \mathbb{T} , and the underlying tree slanted as T . Whenever we say the word *node*, we mean some $t \in T$ in a tree decomposition, and when we say *vertex*, it means some $v \in V$ of the graph G being studied. We write T_t for the *subtree* of T rooted at $t \in T$, that is the tree that contains t and all its descendants. An important consequence of Axiom (T3) that will be relevant later is the following: if a vertex or an edge is contained in both T_c and $T_{c'}$, where c, c' are two distinct children of t , then it must also be contained in the parent node t .

1. Treewidth

For any graph G , there are generally many tree decompositions: we denote this collection $\mathcal{T}(G)$. However, not all of them are useful, e.g. the trivial case of a single node containing the entire graph G . The following definition captures how good a tree decomposition is.

Definition IV.2 (treewidth [2, 16]). For a tree decomposition $\mathbb{T} = (T, \rho, \kappa)$, we define its *treewidth* as:

$$\text{tw}(\mathbb{T}) := \max_{t \in T} \{|\rho(t)| + |\kappa(t)|\} - 1, \quad (21a)$$

that is the size of the *largest* node t in terms of its contents, minus one. For a graph G , we define its treewidth as:

$$\widehat{\text{tw}}(G) := \min_{\mathbb{T} \in \mathcal{T}(G)} \text{tw}(\mathbb{T}), \quad (21b)$$

that is the minimum treewidth of any possible tree decomposition of G . We distinguish the treewidth of a graph with a hat.

The treewidth measures how different a graph is from a tree, and we define the RHS of (21a) with -1 so that a tree Q has $\widehat{\text{tw}}(Q) = 1$.

Both in tensor network contraction and in our permanent computations the running time and memory requirements scale exponentially with the treewidth of the graph. Computing with tree-like graphs is in general much easier than graphs with higher treewidth which contain many cycles [16]. In our case, the intuition is that a graph with high treewidth, and thus many cycles, allows many perfect matchings, i.e. summands of the permanent, which leads to a more expensive computation.

B. Permanent algorithm

We now present the permanent algorithm by Cifuentes and Parrilo from [2, Algorithm 2], to which we refer as

Algorithm CP: Bipartite permanent

Input:

- a matrix $M \in \mathbb{C}^{n \times n}$,
- a tree decomposition $\mathbb{T} = (T, \rho, \kappa)$ of $G(M)$

Result: the permanent per M

```

1 order ← list of nodes in T, in topological order,
  starting from leaves
2 for t ∈ order do
3   Q[t](R, C) ← per M|R, C for R ⊆ ρ(t) and C ⊆ κ(t)
4   if t is a leaf, i.e. ch(t) = ∅ then
5     P[t] ← Q[t]
6   else
7     for cj ∈ ch(t) do
8       { Δcjρ ← ρ(cj) \ ρ(t)   { Δcjκ ← κ(cj) \ κ(t)
       { Λcjρ ← ρ(cj) ∩ ρ(t)   { Λcjκ ← κ(cj) ∩ κ(t)
9       for R ⊆ Λcjρ and C ⊆ Λcjκ do
10        Q'[t|cj](R, C) ← (-1)|R| · Q[t](R, C)
11        Q''[t ← cj](R, C) ←
          P[cj](R ∪ Δcjρ, C ∪ Δcjκ)
12        for R ⊆ ρ(t) and C ⊆ κ(t) do
13          P[t](R, C) ← subset convolution as in (26)
14 return P[r](ρ(r), κ(r)) = per M where r = root(T)

```

FIG. 6. Pseudocode of the Cifuentes and Parrilo algorithm for computing the permanent of a sparse matrix using a tree decomposition of its graph

Algorithm CP, and whose pseudocode can be found in Fig. 6. The algorithm exploits the structure and sparsity of the matrix to accelerate the computation of its permanent. Using a tree decomposition of the graph of the matrix, it is able to decompose the matrix into smaller parts and compute their permanents. The tree structure then tells it how to join these parts together. It is a dynamic programming algorithm that stores values in tables for later use. For an $n \times n$ matrix and a tree decomposition of its graph of treewidth ω , the running time of CP is $\mathcal{O}(n2^\omega\omega^2)$. The running time is conventionally given as $\tilde{\mathcal{O}}(n2^\omega)$, which hides polynomial factors in ω , but the factor ω^2 can be recovered from [2, Lemma 2 and proof of Lemma 14] as detailed in Appendix C.

The Algorithm CP builds the permanent of matrix M from leaves upward. For all nodes and for the steps between child and parent nodes, we need to build two dynamic programming tables $Q[t](R, C)$ and $P[t](R, C)$, both indexed by a subset of rows R and of columns C belonging to a node t . The table Q stores the permanents of rows and columns belonging to the node t , while the table P allows to combine that information with the permanents of its children using a subset convolution described below. In what follows we write $\text{per}_M(R, C)$ for the permanent of a submatrix of M with rows R and columns C .

² We could add also a fourth axiom to disallow degeneracy: for two nodes t and t' , we cannot have both $\rho(t) = \rho(t')$ and $\kappa(t) = \kappa(t')$. This is convenient but not strictly necessary.

1. The local Q -tables

For every node $t \in T$, we have the table of *local permanents* $Q[t](R, C) = \text{per}_M(R, C)$ for all $R \subseteq \rho(t)$ and $C \subseteq \kappa(t)$, i.e. resulting from combinations of row and column vertices contained in the node t . These represent submatrices of M with those rows and columns.

2. The subtree P -tables

Crucial in the construction are the tables of *subtree permanents* $P[t](R, C)$ where $R \subseteq \rho(t)$ and $C \subseteq \kappa(t)$ again, same as in $Q[t]$. Their values are

$$P[t](R, C) = \text{per}_M(R \cup \bar{\Delta}_t^\rho, C \cup \bar{\Delta}_t^\kappa), \quad (22)$$

where $\bar{\Delta}_t^\rho := \rho(T_t) \setminus \rho(t)$, and similarly $\bar{\Delta}_t^\kappa := \kappa(T_t) \setminus \kappa(t)$. The table $P[t]$ stores the permanents of submatrices represented by the entire subtree T_t . Note that the labels of $P[t]$ contain only rows $R \subseteq \rho(t)$ and columns $C \subseteq \kappa(t)$, but the table elements will relate to permanents of submatrices with rows and columns coming from the descendants of t , ensured by $\bar{\Delta}_t^\rho$ and $\bar{\Delta}_t^\kappa$. For leaves ℓ , we have $P[\ell] = Q[\ell]$, because they have no descendants. Conversely, the root $r := \text{root}(T)$ contains the final result:

$$P[r](\rho(r), \kappa(r)) = \text{per}_M(\rho(T), \kappa(T)) = \text{per } M. \quad (23)$$

In (23), the equality follows from the Axiom (T1), which says that $\rho(T)$ is the set of all rows of the (whole) matrix M , and similarly $\kappa(T)$ is the set of all columns.

Note IV.3. We remark on the notational distinction between $\bar{\Delta}_t^\rho$ (resp. $\bar{\Delta}_t^\kappa$) in this section and $\Delta_{c_j}^\rho$ (resp. $\Delta_{c_j}^\kappa$) in the pseudocode in Fig. 6. While the former (with bar) corresponds to the entire subtree of t , the latter (without bar) corresponds to individual children of t and is defined in the following section.

3. Helper tables

The table $P[t]$ of an internal node t is computed using the P -tables of the children of t in a subset convolution. This requires computing helper tables shown below, however, these do not need to be stored for future computation. The first table $Q'[t|c_j]$ is associated to permanents of submatrices made of rows and columns in t that are shared with its child c_j :

$$Q'[t|c_j](R, C) = (-1)^{|R|} Q[t](R, C), \quad (24a)$$

where $R \subseteq \Lambda_{c_j}^\rho := \rho(c_j) \cap \rho(t)$ and $C \subseteq \Lambda_{c_j}^\kappa := \kappa(c_j) \cap \kappa(t)$.

The table $Q''[t \leftarrow c_j]$ brings permanents of submatrices from the child's table $P[c_j]$ up the tree and makes them available to node t . The values transferred are those that correspond to submatrices with rows and columns contained in c_j but not in t , together with a selection of

rows $R \subseteq \Lambda_{c_j}^\rho$ and columns $C \subseteq \Lambda_{c_j}^\kappa$ shared by the two nodes. These index the table:

$$Q''[t \leftarrow c_j](R, C) = P[c_j](R \cup \Delta_{c_j}^\rho, C \cup \Delta_{c_j}^\kappa), \quad (25)$$

where $\Delta_{c_j}^\rho := \rho(c_j) \setminus \rho(t)$ and $\Delta_{c_j}^\kappa := \kappa(c_j) \setminus \kappa(t)$.

We shortly revisit Note IV.3. Recall the P -tables in (22) reference rows $\bar{\Delta}_t^\rho$ (resp. columns $\bar{\Delta}_t^\kappa$) corresponding to the whole subtree T_t . In (25), the helper table $Q''[t \leftarrow c_j]$, the device used to connect t to its subtree, only references the sets $\Delta_{c_j}^\rho$ (resp. $\Delta_{c_j}^\kappa$) corresponding to the immediate children of t . The reason is that the permanents stored in $P[t]$ are obtained recursively using the tree structure, computed from partial permanents stored in the tables $P[c_j]$ of the children c_j which are computed before $Q''[t \leftarrow c_j]$. This justifies the definition (25).

4. Subset convolution

The final step in computing a value of $P[t](R, C)$ for any internal node t (including root) is to perform the *subset convolution* over R and C of all the prepared tables: the local table $Q[t]$, and the helpers $Q'[t|c_j]$ and $Q''[t \leftarrow c_j]$ of all children $c_j \in \text{ch}(t)$. The subset convolution, given in eq. (26) below, computes the value $P[t](R, C)$ as a summation over collections of subsets $\{R_i \subseteq R\}$ and $\{C_i \subseteq C\}$ that partition R and C , respectively. The formula is:

$$\begin{aligned} P[t](R, C) &= \sum_{\{R_i, C_i\}_i} \left(Q[t](R_t, C_t) \right. \\ &\quad \times \prod_{c_j \in \text{ch}(t)} Q'[t|c_j](R_{c_j}, C_{c_j}) \\ &\quad \left. \times Q''[t \leftarrow c_j](\bar{R}_{c_j}, \bar{C}_{c_j}) \right), \end{aligned} \quad (26)$$

Substituting the definitions of the helper tables, the above implements the subset convolution from [2, Lemma 10]. Below, we give a concrete characterization of the subsets $\{R_i, C_i\}$, but first we explain at high level the form of the equation. Each summand in (26) involves all of the tables $Q[t]$, $Q'[t|c_j]$ and $Q''[t \leftarrow c_j]$ (for all children c_j of t), and the subsets $\{R_i, C_i\}$ index those tables. We combine values stored in the tables Q, Q', Q'' for particular submatrices that are selected using the subsets $\{R_i, C_i\}$. These table values are used to compute terms of the permanents stored in $P[t](R, C)$.

Each partition of rows $\{R_i \subseteq R\}$, resp. columns $\{C_i \subseteq C\}$, consists of:

$$\begin{aligned} R_t \sqcup R_{c_1} \sqcup \bar{R}_{c_1} \sqcup \dots \sqcup R_{c_k} \sqcup \bar{R}_{c_k} &= R, \\ C_t \sqcup C_{c_1} \sqcup \bar{C}_{c_1} \sqcup \dots \sqcup C_{c_k} \sqcup \bar{C}_{c_k} &= C, \end{aligned}$$

where k is the number of children of t . Analogously, for columns, we have . The constraints on what those individual subsets may be are given by the following: Let

S be one of the above tables (e.g. $Q'[t|c_j]$ for some child c_j). If for some $R' \subseteq R$ and $C' \subseteq C$, the value $S(R', C')$ is not defined, we assume $S(R', C') = 0$ or equivalently, we exclude the corresponding partitions from the summation. This reasoning gives us the following constraints on the subsets $\{R_i, C_i\}_i$ in the partitions for possibly nontrivial terms of (26):

Recall that $Q[t]$ is defined for sets of rows and columns contained in t , so

$$R_t \subseteq \rho(t) \quad \text{and} \quad C_t \subseteq \kappa(t).$$

Similarly, $Q'[t|c_j]$ and $Q''[t \leftarrow c_j]$ are defined for

$$R_{c_j}, \bar{R}_{c_j} \subseteq \Lambda_{c_j}^\rho \quad \text{and} \quad C_{c_j}, \bar{C}_{c_j} \subseteq \Lambda_{c_j}^\kappa,$$

respectively.

V. PRELIMINARIES TO THE ALGORITHMS

Before we can construct our main contribution, an algorithm for polytime classical simulation of Boson Sampling from shallow interferometers, we need a few more necessary preliminaries. These include the formal definition of the nearest-neighbour circuits in Section V A and the study of their structure when we restrict the depths in Section V B. Then in Section V C, we show how to use the latter structure to construct efficient tree decompositions. Finally, in Section V D, we define a way to represent important matrix concepts, specifically the selection of a submatrix and a column permutation needed for the algorithm CC-C, using tree decompositions.

A. Nearest-neighbour circuits

We are interested in architectures of ideal interferometric circuits composed of nearest-neighbour interactions between modes. It is well known that such interferometers can be constructed from beamsplitters and phase-shifters [17, 18] which are, respectively, two- and one-mode gates. Similarly to [19], we absorb the phase-shifters, being single-mode operations, into adjacent beamsplitters whenever possible.

Definition V.1 (universal beamsplitter [20]). A *beamsplitter* acts on two modes and is represented as:

$$B(\theta, \phi_T, \phi_R) = \begin{pmatrix} e^{i\phi_T} \cos \theta & e^{i\phi_R} \sin \theta \\ -e^{-i\phi_R} \sin \theta & e^{-i\phi_T} \cos \theta \end{pmatrix}. \quad (27)$$

It is parametrised by three angles: the coupling between the two modes θ , transmitted phase shift ϕ_T and reflected phase shift ϕ_R .

We consider a construction with the beamsplitters arranged in alternating layers as displayed in Figure 7, as in the Clements rectangular decomposition [21] that guarantees the universality of the interferometric circuit while

minimizing its depth. This decomposition also has practical advantages, as it guarantees more uniform losses among the different output modes which limits the effects of those imperfections. A full circuit is composed as an alternation of two slightly different families of layers of beamsplitters, L_0 and L_1 , that allows the spreading of the correlations over distant modes following a causal cone.

Definition V.2 (Beamsplitter layer L^0). We define a *beamsplitter layer* $L_{\underline{\Psi}}^0$ parametrized by $\underline{\Psi} = (\underline{\theta}, \underline{\phi}_T, \underline{\phi}_R)$, where $\underline{\theta} = (\theta^1, \dots, \theta^k)$, and similarly $\underline{\phi}_T, \underline{\phi}_R$. These parameters describe all beamsplitters of the layer over the m modes:

$$L_{\underline{\Psi}}^0 := B(\theta^1, \phi_T^1, \phi_R^1) \oplus \dots \oplus B(\theta^k, \phi_T^k, \phi_R^k) \quad (\oplus \mathbb{1}). \quad (28)$$

The number of beamsplitters is $k = \lfloor \frac{m}{2} - 1 \rfloor$, and the $(\oplus \mathbb{1})$ represents the fact that the last term $\mathbb{1}$ is only present when m is odd.

Definition V.3 (Beamsplitter layer L^1). Similarly to the above, we define a *beamsplitter layer* $L_{\underline{\Psi}}^1$ acting on m modes as

$$L_{\underline{\Psi}}^1 := \mathbb{1} \oplus B(\theta^1, \phi_T^1, \phi_R^1) \oplus \dots \oplus B(\theta^k, \phi_T^k, \phi_R^k) \quad (\oplus \mathbb{1}), \quad (29)$$

where $k = \lfloor \frac{m}{2} - 1 \rfloor$, and where $(\oplus \mathbb{1})$ represents the fact that the last term $\mathbb{1}$ is only present when m is even.

An interferometric circuit of depth D consist of a series of L^0 and L^1 beamsplitter layers as represented in Figure 7, where the unitary matrix of the whole circuit is the composition of D alternating layers parametrized by $\{\underline{\Psi}_i\}_i$ and starting with $L_{\underline{\Psi}_1}^0$:

$$\mathcal{U} = L_{\underline{\Psi}_D}^{(D-1) \bmod 2} L_{\underline{\Psi}_{D-1}}^{(D-2) \bmod 2} \dots L_{\underline{\Psi}_2}^1 L_{\underline{\Psi}_1}^0.$$

B. Banded matrices

We will see that restricting the number of layers in the preceding definition, we obtain interferometers represented by banded matrices. We define this notion below:

Definition V.4 (banded matrix). A matrix \mathcal{U} is *banded* if there exist nonnegative integers w_1, w_2 called *lower* and *upper bandwidths*, respectively, such that for all i, j , if $i - j > w_1$ or $j - i > w_2$ then the matrix element $\mathcal{U}_{i,j} = 0$.

We can understand the above as saying that each row (or column) of a banded matrix has at most w_1 nonzero entries below the diagonal, and at most w_2 above the diagonal. In total, each row (column) has at most

$$w_1 + w_2 + 1 =: w$$

nonzero entries, where the $+1$ takes into account the diagonal element. We call w the *bandwidth*. Note the similar terminology *bandwidth(s)* for w and (w_1, w_2) ; this

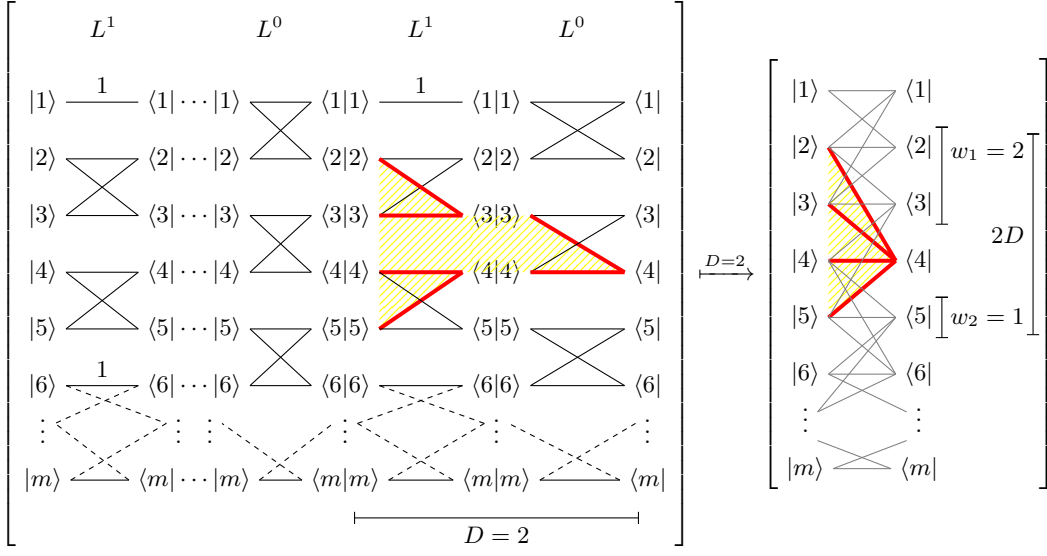


FIG. 7. Alternating arrays of beamsplitters in our architecture. This example is for even depth D (so the last, leftmost, layer is the odd L_1). We represent it using the graphical notation from Fig. 2; note that to keep it consistent with the outer product interpretation, the input is on right and output on the left side. The crossings are beamsplitters. For each mode one beamsplitter connects it with the mode above, and the next beamsplitter with the mode below, or vice-versa. The columns represent the layers of gates L^0 and L^1 . The red lines show the possible paths of photons starting in mode 4, corresponding to its *causal cone* (filled yellow), over two layers of the circuit. The RHS is the corresponding graph resulting from the two first layers of the circuit with the causal cone of mode 4 in yellow.

will not cause confusion, as in our usage, we always write also the symbol.

Figure 7 depicts the interferometer \mathcal{U} composed of D alternating L^0 and L^1 layers of two-mode gates (LHS) and its associated resulting graph $G(\mathcal{U})$ in the example case of $D = 2$ (RHS). Observe that the nearest-neighbour interaction and the alternation of layers L^0 and L^1 impose that w_1, w_2 can only increase by at most one for each added layer. This is consistent with the result in [21] that depth $D = m$ is required to generate an arbitrary unitary \mathcal{U} .

Lemma V.5 (bandwidth). *The bandwidth w of a circuit composed of D alternating L^0 and L^1 layers satisfies the condition:*

$$w = w_1 + w_2 + 1 \leq 2D. \quad (30)$$

Note that (30) is an inequality because some beamsplitters may act as a diagonal matrix, producing no coupling between the modes. This happens when the coupling angle $\theta = 0$ or π .

Proof of Lemma V.5. We use the help of Figure 7, and we show how the widths grow as we increase the depth D by adding the appropriate beamsplitter layers. We proceed by induction on D . For simplicity, we assume generic coupling angles, i.e. ignoring the cases where $\theta = 0, \frac{\pi}{2}, \pi, \dots$, because we are interested in the maximum possible connectivity between input and output modes. Likewise, we ignore the edge cases of 1×1 identity blocks

at the first or last mode. These simplifications allow us to focus on the main idea, but do not obscure the full picture.

a. Base case: $D = 1$. A single layer L^0 or L^1 is, by construction, a matrix with 2×2 blocks on the diagonal. In Figure 7, in the first (rightmost) layer of the LHS, observe that input modes are partitioned into pairs of nearest neighbours, and coupling is only possible within these pairs. Thus the output modes of the layer are also partitioned correspondingly. Conclude that the maximum number of nonzero elements in a row or columns is $w = 2 = 2D$.

b. Induction hypothesis: Suppose for D layers, we have bandwidth $w \leq 2D$. The last beamsplitter layer is $L_{\Psi_D}^{(D-1) \bmod 2}$. We add a new layer $L_{\Psi_{D+1}}^{D \bmod 2}$, which is of different type than the previous. The new layer also acts on disjoint pairs of nearest-neighbor modes, but it is shifted by one mode in comparison to the previous layer. Observe in Figure 7 that this, in general, expands the maximum reach of any given input mode by two more output modes: one upward (lower index) and one downward (higher index),³ i.e. the new bandwidth is bounded as:

$$w' \leq w + 2 \leq 2(D + 1).$$

³ **NB:** We are ignoring the edge case when there are no more modes to expand into. Of course, the inequality on bandwidth still holds.

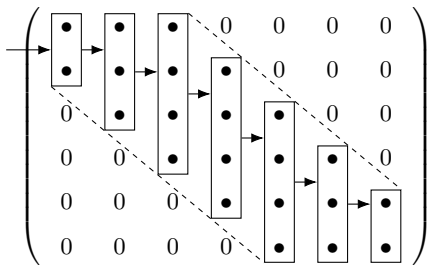


FIG. 8. Example of linear tree decomposition T^C where tree nodes correspond to parts of columns of the matrix. The nodes are shown as boxes that encompass the possibly nonzero elements, signified by bullets “•”. The dashed lines show the band.

Together, paragraphs a and b prove the Lemma by induction. ■

C. Tree decomposition of a banded matrix

There are different tree decomposition one can design for an $m \times m$ banded matrix \mathcal{U} . For algorithmic design and simplicity we will use a linear tree decomposition $T^C = (T, \rho, \kappa)$ shown in Figure 8 that is not optimal but simple.⁴ The decomposition T^C consists of a linear tree $T = \{t_1, \dots, t_m\}$ where the node t_i has a single child t_{i+1} for $i = 1, \dots, m-1$, and there is a correspondence between the nodes and columns of the matrix, such that $\kappa(t_i) = \{i\}$ for all $i \in [m]$. This tree decomposition associates to each node t_i , corresponding to column i , all rows j where the matrix elements of that column is nonzero: $|j\rangle \in \rho(t_i)$ iff $\mathcal{U}_{ji} \neq 0$. If \mathcal{U} has bandwidths (w_1, w_2) , then in general:

$$\rho(t_i) = \{|j - w_1\rangle, |j - w_1 + 1\rangle, \dots, |j + w_2\rangle\}, \quad (31)$$

apart from cases where this would include nonexistent row labels, i.e. $|j\rangle$ for $j \notin \{1, \dots, m\}$. There are at most $w = w_1 + w_2 + 1$ elements in $\rho(t_i)$, and together with a single element in $\kappa(t_i)$, recalling that the treewidth is defined with a constant -1 (see (21a)), this makes the treewidth of the decomposition $\text{tw}(T^C) = w \leq 2D$. The inequality follows from Lemma V.5.

D. Modification of the tree decomposition

Having a low-width tree decomposition, we are able to compute the permanent of a matrix efficiently using

⁴ The optimal decomposition uses two nodes per column, each containing w rows, where $w + 1$ is the number of rows with a nonzero in a column. These nodes are neighbours, one containing the upper w rows, and the other the lower. This was given by Cifuentes and Parrilo [2], modulo exchange of rows and columns between their paper and ours.

Algorithm CP. However, while the original matrix has a banded structure allowing us to find the decomposition, this structure is concealed when we permute columns and take submatrices (delete rows and columns), transformations required by the the CC sampling algorithms. In principle, we need a new tree decomposition for each submatrix or column permutation, and these are no longer easy to find. However, in what follows we present a systematic approach to obtain all tree decompositions of submatrices needed for our sampling algorithm from the initial tree decomposition of the whole banded matrix \mathcal{U} by performing a set of simple manipulations. This approach has the practical advantage of constructing the tree decomposition in a simpler and more efficient way.

We proceed in three sections: In Section VD1, we deal with column permutations by observing that they simply rename the labels of the graph of the matrix. Then in Section VD2, we define the notion of tree restriction which represents a submatrix, viewed as restricting the row and column labels that are associated to nodes. Furthermore, we bound the treewidth of such restriction. Note that these results, on permutations and submatrices, apply to general tree decompositions, beyond the linear trees used in our algorithm for banded matrices.

Finally, in Section VD3, we observe that a tree restriction may render some nodes redundant, and we show that these may then be removed from the tree in the appropriate way without changing the value of the corresponding permanent. This last fact will be important for our manipulations of the tree decomposition within our sampling algorithm in Section VIB.

1. Permutation of columns

An important step of both Algorithm CC-C and our algorithm is to choose a uniformly random permutation of all input qudits. This permutation is selected independently for each sample generated. In CC-C, the permutation is used to permute columns of the matrix. We show below that this has the effect of relabeling the input (column) labels in our tree decomposition.

Lemma V.6 (column permutation). *Let $T = (T, \rho, \kappa)$ be a tree decomposition corresponding to an $m \times n$ matrix M . Let $\alpha \in S_n$ be a permutation, and let M' be a $m \times n$ matrix with elements $M'_{i,j} = M_{i,\alpha(j)}$. This has the same columns as M , but their order is given by α .*

Let $T' = (T, \rho, \kappa')$ be a tree decomposition with the same tree and row labels as T , but with column labels:

$$\kappa'(t) := \{ \langle \alpha^{-1}(j) | \mid |j\rangle \in \kappa(t) \}$$

for each node $t \in T$. Then T' is a tree decomposition of M' .

Proof. We show this in terms of $G(M')$, the bipartite graph of the matrix M' , which comes from the view of

M' as a sum of outer products; see Fig. 2. The permuted matrix is:

$$\begin{aligned} M' &= \sum_{i,j} M'_{i,j} |i\rangle\langle j| \\ &= \sum_{i,j} M_{i,\alpha(j)} |i\rangle\langle j| = \sum_{i,j} M_{i,j} |i\rangle\langle \alpha^{-1}(j)|. \end{aligned}$$

Permuting the columns of M to obtain M' is equivalent to renaming the vertices of $G(M)$ corresponding to columns by α^{-1} while keeping the connectivity and edge weights the same. This action is a graph isomorphism. Renaming those same vertices as contents of the tree decomposition T to obtain T' ensures that T' is a tree decomposition of $G(M')$. ■

2. Submatrices

A central tool of the Clifford and Clifford sampling algorithms is computation of permanents of submatrices of a larger matrix. To achieve this more efficiently using tree decompositions, we define below a notion of restriction of the original tree. As seen in an example in Figures 9a and 9b, intuitively, this corresponds to deleting labels from within the nodes of the tree.

Definition V.7 (tree restriction). Let $T = (T, \rho, \kappa)$ be a tree decomposition of the graph $G(\mathcal{U}) = (V = \mathcal{R} \sqcup \mathcal{C}, E)$, and let $\mathcal{R}' \subseteq \mathcal{R}$ and $\mathcal{C}' \subseteq \mathcal{C}$ be subsets of rows and columns, respectively. Define the *restriction* of T to those subsets as $T|_{\mathcal{R}', \mathcal{C}'} = (T, \rho', \kappa')$. It has the same tree T , but the contents of its nodes are given by $\rho' : T \rightarrow 2^{\mathcal{R}'}$ and $\kappa' : T \rightarrow 2^{\mathcal{C}'}$ which are defined as $\rho'(t) = \rho(t) \cap \mathcal{R}'$ and $\kappa'(t) = \kappa(t) \cap \mathcal{C}'$ for all $t \in T$.

This tree restriction is a valid representation of the equivalent restriction of the matrix, that is the submatrix with the selected rows and columns. Formally:

Lemma V.8. *In the above notation, the restriction $T|_{\mathcal{R}', \mathcal{C}'}$ is a tree decomposition of the submatrix $\mathcal{U}|_{\mathcal{R}', \mathcal{C}'}$ of \mathcal{U} that has rows \mathcal{R}' and columns \mathcal{C}' .*

Sketch proof. We start with T which is a tree decomposition of the graph $G(\mathcal{U})$. To obtain the submatrix $\mathcal{U}' \equiv \mathcal{U}|_{\mathcal{R}', \mathcal{C}'}$, we remove rows and columns from \mathcal{U} , and we remove those same row and column labels from T , without changing anything else, to obtain $T' \equiv T|_{\mathcal{R}', \mathcal{C}'}$. This means that T' contains all the necessary row and column labels to describe \mathcal{U} (satisfies Axiom (T1)). Furthermore, the row and columns labels that remain in T' are preserved in all the relevant nodes, which means all edges corresponding to nonzero elements of \mathcal{U}' are captured by T' (Axiom (T2)), and that the connectivity requirement (Axiom (T3)) between the nodes of T' is also satisfied. Informally, the latter two facts hold for T' because they hold T and the restriction preserves enough structure.

We present a formal proof in Appendix D 1: this consists of explicitly verifying that T' satisfies the axioms of a tree decomposition with respect to $\mathcal{U}|_{\mathcal{R}', \mathcal{C}'}$. ■

An important fact is that the restriction produces a tree decomposition that is no worse than the original:

Lemma V.9 (treewidth). *Using previous notation, the treewidth of the restriction is bounded as*

$$\text{tw}(T|_{\mathcal{R}', \mathcal{C}'}) \leq \min(\text{tw}(T), |\mathcal{R}'| + |\mathcal{C}'| - 1). \quad (32)$$

Proof. A restriction may only remove vertices from the decomposition, so the treewidth can only decrease, i.e. $\text{tw}(T|_{\mathcal{R}', \mathcal{C}'}) \leq \text{tw}(T)$. Treewidth measures the size of the largest node, and that cannot be larger than $|\mathcal{R}'| + |\mathcal{C}'|$, i.e. the total number of vertices left. Recall from (21a) that treewidth is one less than the size of largest node. In general, we cannot know which of the choices $\text{tw}(T)$ or $|\mathcal{R}'| + |\mathcal{C}'| - 1$ will be lower, hence we keep the minimum operator. ■

Finally, we note that the tree restriction $T|_{\mathcal{R}', \mathcal{C}'}$ is not necessarily the best decomposition of $\mathcal{U}|_{\mathcal{R}', \mathcal{C}'}$: Lemma V.9 only shows the upper bound on its treewidth. However, crucially, the restriction is easy to find even when an optimal decomposition may not be, e.g. due to column permutations, or if we need a submatrix of a submatrix of \mathcal{U} . Furthermore, as the restriction requires nothing more than taking two set intersections at each node of the tree, it is efficient to compute.

3. Redundancy of nodes

As defined in Section V C, each node of our tree decomposition contains a single column label. When restricting the decomposition to $T' = (T, \rho', \kappa')$, we may end up with a node $t \in T$ without any columns, i.e. $\kappa'(t) = \emptyset$. Indeed, our algorithm will perform such restrictions extensively. In the following Lemma V.10, we prove that in this case, deleting this node and connecting its neighbours in the appropriate way leads to a new tree decomposition, denoted $T \setminus t$, that still gives the correct permanent.

In the case of linear trees (no branching), which are those we use in our algorithm, if t is an internal node with a single child, let p, c be the parent and child of t , respectively. Then $T \setminus t$ is a decomposition without the node t where p is connected directly to c . If t is the root (has no parent), then just make its child c the new root in $T \setminus t$. If t is a leaf, just delete it. We present an example in Figures 9c and 9d.

Below, we show that this preserves the permanent by proving that both T and $T \setminus t$ represent the same matrix. Intuitively, in terms of Algorithm CP, the tables $Q[t]$ and $Q'[t|c_j]$ of node t (and its child c_j) become trivial, and the tables $Q''[t \leftarrow c_j]$ and $P[t]$ only act to bring data from the child of t up the tree, making them accessible to the

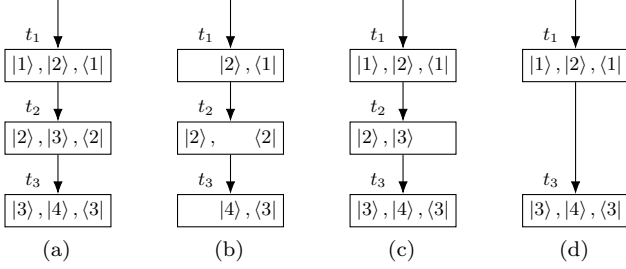


FIG. 9. Example of a linear tree decomposition, of the form from Figure 8, and its restrictions. **(a)** The original tree decomposition T . **(b)** A restriction $T|_{\mathcal{R}', \mathcal{C}'}$ to rows $\mathcal{R}' = \{|2\rangle, |4\rangle\}$ and columns $\mathcal{C}' = \{|1\rangle, |2\rangle, |3\rangle\}$. Observe that vertices $|1\rangle$ and $|3\rangle$ of the underlying graph have been removed. **(c)** Another restriction, this time only removing the column $|2\rangle$. Note that this makes the middle node t_2 redundant because it contains no column label, so it cannot contribute any new elements from the matrix. Instead, node t_2 is only used to copy some of the values from the P -table of t_3 and bring them up the tree, making them available to t_1 . Following Lemma V.10, the permanent computed from this tree decomposition is the same as the one from: **(d)** The new tree decomposition $T \setminus t_2$, where we remove node t_2 , and connect t_1 directly to t_3 instead.

parent of t . Thus we may use $T \setminus t$ instead of T in our permanent calculation.

Lemma V.10 (redundant nodes). *Let $T = (T, \rho, \kappa)$ be a tree decomposition of the graph of a matrix M , where T is a linear tree. Suppose there is a node $t \in T$ such that $\kappa(t) = \emptyset$ and $\rho(t) \subseteq \rho(T \setminus t)$. Then $T \setminus t$ also represents the matrix M .*

Intuitively, under the conditions imposed in Lemma V.10, particularly that $\kappa(t) = \emptyset$, the node t cannot give us any new information about the matrix that is not already contained in the rest of the tree. We give a formal proof in Appendix D 2. There, we also explain the reason why we need the second, subtle but important condition that $\rho(t) \subseteq \rho(T \setminus t)$ (see Note D.2). In short, if there exists a row in $\rho(t)$ not contained also elsewhere in the tree (i.e. $\rho(t) \not\subseteq \rho(T \setminus t)$), then this means there is a row of all zeros in the matrix, and consequently $\text{per } M = 0$. Then the node t cannot be removed from the tree decomposition, because $T \setminus t$ would compute the wrong (non-zero) permanent.

VI. ALGORITHM FOR SHALLOW CIRCUITS

We now have all the tools necessary to enhance the Algorithm CC-B for Boson Sampling simulation for low-depth banded or column-sparse unitaries. The idea is to compute the $\{\text{per } \mathcal{W}_{\circ i}\}_i$ in CC-B using restrictions of initial tree-decomposition of the graph $G(\mathcal{U})$ of the circuit unitary \mathcal{U} . This allows the replacement of the exponential dependency on the number of photons n by the

dependency on the treewidth ω , leading to a running time $\mathcal{O}(mn^2\omega^22^\omega)$ replacing the less efficient term $\mathcal{O}(mn2^n)$. A similar method was used before in [11].

In the following, we show how one can replicate the benefit of using the Laplace expansion in Clifford and Clifford's algorithm CC-C to remove the scaling of m , which is a non-negligible practical improvement considering that the non-collision condition imposes $m = \Omega(n^2)$.

A first attempt would be to independently compute the $k+1$ permanents of submatrices $\mathcal{W}_{\circ i}$ needed in the Laplace expansion (19b) of the marginal of size $k+1$ in Algorithm CC-C. Unfortunately, this would lead to a scaling $\mathcal{O}(n^3\omega^22^\omega)$ to compute all of $\{\text{per } \mathcal{W}_{\circ i}\}_i$.

In the following sections, we show how to achieve $\mathcal{O}(n^2\omega^22^\omega)$ by finding an efficient way of computing those $k+1$ permanents of submatrices \mathcal{W}_i° using a single tree decomposition, leading to a scaling linear in k , reproducing the saving obtained in the original proposal of Clifford and Clifford. The key tool is to compute the $k+1$ permanents of submatrices $\mathcal{W}_{\circ i}$ by doing local updates to the single initial (restricted) tree decomposition. This will allow us to exploit precomputed tables, reducing the amount of required computation at each step, closely mimicking the idea of Clifford and Clifford.

We proceed in several steps, referencing the pseudocode of our Algorithm 1 from Figure 10. In Section VI A, we prepare the tree decomposition of \mathcal{U} , including the selection of only the occupied input modes, i.e. the restriction to certain columns, as well as the permutation thereof. In Section VI B, we explain the sampling algorithm itself, showing how to sample the first two marginals, and then we generalize to an arbitrary marginals. Finally in Section VI C, we show that the asymptotic running time of our algorithm is $\mathcal{O}(n^22^\omega\omega^2) + \mathcal{O}(\omega n^3)$.

A. Preparation

Before we can start generating the sample, we first need to prepare the main tree decomposition. This corresponds to lines 1 to 4 in the pseudocode in Figure 10.

We create a linear tree-decomposition $T = T^C$ of the graph $G(\mathcal{U})$ associated to the banded unitary \mathcal{U} , where each tree node contains a single column label (input of the circuit) and all row labels (outputs of the circuit) for which that column has a non-zero element in \mathcal{U} . This is the decomposition defined in Section V C.

We have a fixed pattern of input photons to the circuit $|\underline{n}\rangle$ with $n_i \in \{0, 1\}$ for each input mode i . We restrict the tree decomposition T by removing the columns corresponding to unoccupied input modes. We also remove those rows that only contain zeros after the deletion of columns. The new decomposition \tilde{T} corresponds to the submatrix $\mathcal{V}^{\underline{n}}$ of \mathcal{U} restricted to the columns corresponding to occupied inputs, see Lemma V.10. The matrix $\mathcal{V}^{\underline{n}}$ may apparently have different band structure, but this is not a problem: the original structure is preserved in the restricted tree-decomposition whose treewidth remains at

Algorithm 1: Boson Sampling using tree decomposition and tree rotations

Input:

- an $m \times m$ matrix \mathcal{U} representing a shallow interferometer on m modes of depth D ,
- a positive integer n , the desired sample size

Result: a single sample \underline{n}'

// preparation, see Section VI A

- 1 $\alpha \leftarrow$ uniformly random permutation from S_n ;
 - 2 $\mathcal{V}^{\underline{n}} \leftarrow$ first n columns of \mathcal{U} , permuted using α s.t. $\mathcal{V}_{i,j}^{\underline{n}} = \mathcal{U}_{i,\alpha(j)}$;
 - 3 $\tilde{T} = (T, \rho, \kappa) \leftarrow$ linear tree decomposition of $G(\mathcal{V}^{\underline{n}})$ as described in Section VI A, with $T = \{t_1 \rightarrow t_2 \rightarrow \dots \rightarrow t_n\}$, rooted in t_1 , with column labels $\kappa(t_j) = \{\langle \alpha^{-1}(j) | \}$, and with row labels $\rho(t_j) = \{|i\rangle \mid \mathcal{U}_{i,\alpha(j)} \neq 0\}$; note this already includes the column permutation ;
 - 4 prepare all Q tables in \tilde{T} : for t_j and for $|i\rangle \in \rho(t_j)$, we have $Q[t_j](\{|i\rangle\}, \{\langle \alpha^{-1}(j) | \}) \leftarrow \mathcal{V}_{i,j}^{\underline{n}}$, $Q[t_j](\emptyset, \emptyset) \leftarrow 1$, and all others 0;
// first photon, see Section VIB 1
 - 5 $p_1(i) \leftarrow |\mathcal{U}_{i,\alpha(1)}|^2$ where $\mathcal{U}_{i,\alpha(1)} = Q[t_{\alpha(1)}](\{|i\rangle\}, \{\langle 1 | \})$, for $|i\rangle \in \rho(t_{\alpha(1)})$;
 - 6 $r_1 \leftarrow$ sample from pmf p_1 ;
// expanding the sample to k photons, see Section VIB 2
 - 7 for $k \leftarrow 2, \dots, n$ do
 - 8 construct the restriction T^{W} of \tilde{T} to rows $\{|r_1\rangle, \dots, |r_{k-1}\rangle\}$ and columns $\{\langle 1 |, \dots, \langle k | \}$; this contains only nodes $t_{\alpha(1)}, \dots, t_{\alpha(k)}$, connected as in \tilde{T} ; we denote its tree nodes $\{\hat{t}_1 \rightarrow \dots \rightarrow \hat{t}_k\}$ for convenience (see Note VI.3), and we denote its row function $\hat{\rho}$;
// iterate over the possible choices of the new mode r_k ; note the use of the unrestricted ρ of \tilde{T}
 - 9 for $i \in \bigcup_{j=1}^k \rho(\hat{t}_j) \setminus \{r_1, \dots, r_{k-1}\}$ do
 - 10 update $\hat{\rho}$ to recover the row $|i\rangle$ in nodes that contain it in the unrestricted decomposition \tilde{T} ;
 - 11 compute the P tables of the subtree of \hat{t}_2 : $P[\hat{t}_k], P[\hat{t}_{k-1}], \dots, P[\hat{t}_2]$ using (26); see fig. 11a ;
// compute the Laplace expansion
 - 12 initialize $L \leftarrow 0$ to hold the running value of the Laplace expansion;
 - 13 for $j \leftarrow 1, \dots, k$ do
 - 14 // manipulate the tree, see Fig. 11
 - 15 set the child of \hat{t}_{j-1} to be \hat{t}_{j-2} , whenever these exist;
 - 16 replace \hat{t}_j with a new dummy d as the root with children \hat{t}_{j-1} and \hat{t}_{j+1} , whenever they exist, and contents $\hat{\rho}(d) = \hat{\rho}(t_{j-1}) \cap \hat{\rho}(t_{j+1})$ and $\hat{\kappa}(d) = \emptyset$;
// compute only tables where this is necessary; this corresponds to yellow nodes in the example Fig. 11b-e
 - 17 compute $P[\hat{t}_{j-1}]$ using (26), if \hat{t}_{j-1} exists;
 - 18 compute $P[d]$ using (26); note that this only depends on $Q[d]$, as well as $P[\hat{t}_{j-1}], P[\hat{t}_{j+1}]$ whenever t_{j-1}, t_{j+1} exist;
// add summand to Laplace expansion:
 - 19 $L \leftarrow L + \mathcal{U}_{r_k, \alpha^{-1}(j)}$ per $\mathcal{W}_{\phi_{\alpha^{-1}(j)}}$ where the values are found as follows:

$$\mathcal{U}_{r_k, \alpha^{-1}(j)} = Q[\hat{t}_j](\{|i\rangle\}, \{\langle \alpha^{-1}(j) | \})$$

$$\text{per } \mathcal{W}_{\phi_{\alpha^{-1}(j)}} = P[d](\hat{\rho}(d), \emptyset)$$

and where $\langle \alpha^{-1} |$ is the single column in $\hat{\kappa}(\hat{t}_j)$;
 - 20 replace d by \hat{t}_j , restoring the tree to a state before line 15;
 - 21 remove $|i\rangle$ in $\hat{\rho}$, undoing line 10;
 - 22 $p_k(i) \leftarrow |L|^2$, the marginal probability that we add mode i ;
 - 23 $r_k \leftarrow$ sample from (possibly unnormalised) pmf p_k ;
 - 24 $\underline{n}' \leftarrow$ count occurrences in \underline{r} , i.e. $n'_i =$ number of i 's in \underline{r} ;
 - 25 return \underline{n}' , corresponding to state $|\underline{n}'\rangle$;
-

FIG. 10. Pseudocode of Algorithm 1

most ω by Lemma V.9.

1. Permutation of inputs

The first step consists of generating a uniformly random permutation α from S_n that we will use to permute the input columns. We relabel the column labels in the tree decomposition \tilde{T} , i.e. replace

$$\langle i | \mapsto \langle \alpha^{-1}(i) |, \quad (33)$$

so that the new tree decomposition corresponds to the matrix with (i, j) -th component given by $\mathcal{V}_{i, \alpha(j)}^{\mathbb{Z}}$ for each i, j . This is the matrix obtained from $\mathcal{V}^{\mathbb{Z}}$ by permuting its columns; see Lemma V.6. Note that after the permutation, the column label $\langle i |$ is found in node $t_{\alpha(i)}$ of the tree.

Note VI.1. We choose the convention in (33) that α acts within the column labels by inverse. This is to keep addressing matrix components by just the (non-inverse) α , e.g. $\mathcal{V}_{i, \alpha(j)}^{\mathbb{Z}}$, which is consistent with our notation in Lemma V.6, as well as in Section III B where we introduce the permutation trick used by CC-B.

Recall from Lemma V.6 that the permutation acts on the graph as an isomorphism from $G(\mathcal{V}^{\mathbb{Z}})$ to itself, only renaming column labels. Likewise, its action on the tree decomposition \tilde{T} is the same renaming of column labels, and thus is an isomorphism of the tree decompositions to itself, preserving the tree and all the associated structure, in particular encoding the same connectivity of the underlying graph. We do not formally define the notion of isomorphisms between tree decomposition because it is rather involved; instead, we emphasize that the only action, on both $G(\mathcal{V}^{\mathbb{Z}})$ and \tilde{T} , is the renaming of columns, and it is the same renaming, so it preserves the structure and the correspondence of \tilde{T} to $G(\mathcal{V}^{\mathbb{Z}})$.

2. Precomputing Q -tables

Furthermore, as part of the preparation, on line 4 we compute the Q tables of the entire tree, for later convenience. As each table $Q[t]$ is local to the node t , each containing $|\kappa(t)| = 1$ column, this consists of permanents of 1×1 matrices, i.e. just components of $\mathcal{V}^{\mathbb{Z}}$. The table $Q[t]$ is constructed by simply copying the appropriate values from the matrix. We need these tables for consistency with the formulation of the Cifuentes and Parrilo algorithm, though in practice, one may choose to not implement the Q tables, and simply refer directly to the matrix.

B. The sampling algorithm

In the following subsections, we describe the sampling algorithm itself. In the pseudocode, this starts at line 5.

In Section VIB 1, we show how to compute the marginal probability for the first photon, which is a simple special case and can be done separately. Then in Section VIB 2, we generalize this to an arbitrary marginal $k > 1$, designing the algorithm based on a sequence of manipulations of the tree decomposition of the circuit unitary.

1. First marginal

In the case of the first marginal, which can be seen as expanding the empty sample to $k = 1$ photon, the Laplace expansion is trivial as the matrix $\mathcal{W}_{\circ 1}$ is empty. Equivalently, we compute the permanents of 1×1 matrices. The probability of the first photon being in output mode i is $p_1(i) = |\mathcal{W}_{1,1}^{(i)}|^2$, where the subscript on p_1 indicates that this is the first marginal. This probability is the modulo-squared value of:

$$\mathcal{W}_{1,1}^{(i)} = \tilde{\mathcal{V}}_{1,1}^{(i), (\alpha(1))} = \mathcal{U}_{i, \alpha(1)}.$$

This is the matrix element represented by the node $t_{\alpha(1)}$ containing the label $\langle 1 |$. We remark that one does not need to explore all m output modes, as at most ω are connected to the input mode $\alpha(1)$ due to the circuit depth. We select one output mode at random, using the computed marginal probability distribution p_1 , and store it in the register r_1 . In the pseudocode in Figure 10, this corresponds to lines 5 and 6.

2. The k -th marginal

In the previous Section VIB 1, we explicitly computed the first marginal probability which had a simple form. Now we generalize to arbitrary marginals, showing how to implement the Laplace expansion of the permanent using tree decomposition machinery. This is the crux of our algorithm. What is more, another advantage reveals itself here: not only can we efficiently compute the permanents needed for the Laplace expansion, but by doing our tree manipulations in the right order, we achieve the ability to reuse almost all dynamic programming tables for several calculations.

The k -th marginal, for $k > 1$, adds the k -th input photon to the sample of $k - 1$ distinct photon modes (r_1, \dots, r_{k-1}) which we have already obtained in previous steps. The latter determine the matrix $\mathcal{W} = \tilde{\mathcal{V}}^{(r_1, \dots, r_{k-1}), \alpha([k])}$ made of the restriction of $\mathcal{V}^{\mathbb{Z}}$ to rows (r_1, \dots, r_{k-1}) , and to columns $\alpha([k])$. The k -th marginal adds one more output photon, leading to $k \times k$ matrices $\mathcal{W}^{(r_k)}$, for all $r_k \in [m] \setminus \{r_1, \dots, r_{k-1}\}$. Recall that $\mathcal{W}^{(r_k)}$ is the matrix obtained from \mathcal{W} by adding a row r_k of $\mathcal{V}^{\mathbb{Z}}$, restricted to the same columns $\alpha([k])$.

The matrix \mathcal{W} is represented by the restriction $T^{\mathcal{W}}$ of \tilde{T} that removes all column labels other than $\langle 1 |, \dots, \langle k |$ which are found in tree nodes $t_{\alpha(1)}, \dots, t_{\alpha(k)}$, respectively. We also need to remove all output labels except

$|r_1\rangle, \dots, |r_{k-1}\rangle$. Note that this is the first time we see node redundancy from Section VD3: all nodes except for $t_{\alpha(1)}, \dots, t_{\alpha(k)}$ are made redundant in this restriction, so we can skip them in the permanent computations. Equivalently, we delete the redundant nodes while keeping the remaining nodes connected, as in Fig. 9d.

The (unnormalized) marginal probability distribution p_k of the k -th photon has values $p_k(r_k) = |\text{per } \mathcal{W}^{(r_k)}|^2$ for each value of r_k . We compute $\text{per } \mathcal{W}^{(r_k)}$ using the Laplace expansion from eq. (19b):

$$\text{per } \mathcal{W}^{(r_k)} = \sum_{j=1}^k \mathcal{U}_{r_k, \alpha(j)} \text{per } \mathcal{W}_{\circ j}.$$

We compute the collection $\{\text{per } \mathcal{W}_{\circ j}\}_{j=1}^k$ of permanents of the shared submatrices using a collection of closely related tree restrictions $\{\mathbb{T}_{\circ j}\}_{j=1}^k$. Each $\mathbb{T}_{\circ j}$ is the restriction of $\tilde{\mathbb{T}}$, the global decomposition of $\mathcal{V}^{\mathbb{Z}}$, to rows $\{r_1, \dots, r_{k-1}\}$ and columns $\alpha([k]) \setminus \{j\}$, that is, $\mathbb{T}_{\circ j}$ is the tree decomposition representing the matrix $\mathcal{W}_{\circ j}$.

2a. The moving head: relations between $\mathbb{T}_{\circ j}$

We could now already compute the Laplace expansion using $\{\mathbb{T}_{\circ j}\}_{j=1}^k$. However, the order in which we compute these permanents matters, and the right choice allows us to reuse the dynamic programming tables in the algorithm of Cifuentes and Parrilo. The strategy will be to view the collection $\{\mathbb{T}_{\circ j}\}_{j=1}^k$ as a sequence of local manipulations to the overarching tree decomposition $\mathbb{T}^{\mathcal{W}}$ corresponding to \mathcal{W} . Recall that this is the restriction of $\tilde{\mathbb{T}}$ to rows $\{r_1, \dots, r_{k-1}\}$ and columns $\alpha([k])$.

An example of our procedure can be seen in Figure 11, where each subfigure corresponds to one of the steps. We conceptualize this as a machine head moving along the nodes of $\mathbb{T}^{\mathcal{W}}$ and performing local manipulations, thus building the Laplace expansion step-by-step. This is in analogy to the head of a Turing machine moving along the tape.

Let (j_1, \dots, j_k) be some permutation of $[k]$ that determines the order in which we compute the permanents, i.e. we start with $\text{per } \mathcal{W}_{\circ j_1}$, continue with $\text{per } \mathcal{W}_{\circ j_2}$, etc. To obtain $\mathbb{T}_{\circ j_1}$ from $\mathbb{T}^{\mathcal{W}}$, we restrict the latter, removing the column j_1 , in analogy to obtaining $\mathcal{W}_{\circ j_1}$ from \mathcal{W} . It will be useful to view this as removing the node $t_{\alpha(j_1)}$ and replacing it with a *dummy* node d that contains no information (which we make precise below in Note VI.2); we can do this because $t_{\alpha(j_1)}$ is made redundant when removing column j_1 (see Section VD3). We use $\mathbb{T}_{\circ j_1}$ to compute $\text{per } \mathcal{W}_{\circ j_1}$ using the CP algorithm; note that this includes among others computing the dynamic programming tables $Q[d]$ and $P[d]$ of d . After we compute the permanent $\text{per } \mathcal{W}_{\circ j_1}$, we return the node $t_{\alpha(j_1)}$ and move on to the next permanent $\text{per } \mathcal{W}_{\circ j_2}$ computed using $\mathbb{T}_{\circ j_2}$, where we again replace $t_{\alpha(j_2)}$ by a *new* dummy, and we iterate this process over all j_1, \dots, j_k .

Note VI.2. Each of these steps j (tree restriction $\mathbb{T}_{\circ j}$; denote its row and column functions ρ', κ' here) gets a new dummy node. However, for simplicity and to emphasize they do not bring new information, we denote them all just d . The dummy contains no columns: $\kappa'(d) = \emptyset$. However, in order for $\mathbb{T}_{\circ j}$ to satisfy Axiom (T3) of tree decompositions, the dummy has to contain those rows that are shared between both of its neighbours, on the left and on the right, whenever both exist. That is, if the tree of $\mathbb{T}_{\circ j}$ has a (connected) subtree $\{t_a \rightarrow d \rightarrow t_b\}$ where t_a, t_b are some nodes, then $\rho'(d) = \rho'(t_a) \cap \rho'(t_b)$. If d is at the edge of the tree, i.e. only has one neighbour, then we set $\rho'(d) = \emptyset$.

The values j_1, \dots, j_k defining the order of permanents above are chosen so that we visit the nodes $t_{\alpha(j_1)}, \dots, t_{\alpha(j_k)}$ in the order as they appear in the tree of $\mathbb{T}^{\mathcal{W}}$, meaning that $t_{\alpha(j_\ell)} = t_\ell$ which implies $j_\ell = \alpha^{-1}(\ell)$ for all ℓ .⁵ Note that we assume we have deleted all other nodes due to being redundant. In the next Sec. VIB2b, we show why this order is useful.

Note VI.3. For simplicity, in Fig. 11, we label the nodes by consecutive numbers as t_1, \dots, t_5 , ignoring the possibility that some nodes of the original $\tilde{\mathbb{T}}$ have been removed, which would make this labelling incorrect (and that perhaps the correct numbering would be for example $t_1, t_2, t_4, t_{10}, t_{11}$). We shall use the same convention also in Section VIB2b.

2b. Moving the root: the reuse of P -tables

We enhance the algorithm further to ensure we can reuse the P -tables for several sub-permanents $\{\text{per } \mathcal{W}_{\circ j}\}_j$ as they are evaluated in the sequence given above. This seems a priori not possible: Recall from Section IVB2 that the table $P[t]$ of a node t depends on the P -tables of the children of t (via the helper tables $Q''[t \leftarrow c]$ for each child c) which means that if any of the P -tables of the children (or, by extension, descendants) of t change, we have to recompute $P[t]$ as well. This makes it impossible to reuse P -tables without adapting the method above.

To formulate the solution below, we switch notation to indexing nodes by their order in the tree as t_j , instead of the heavier notation $t_{\alpha(j)}$ we used in the previous section to more easily address matrix columns. Remark that the node t_j corresponds to the column $\alpha^{-1}(j)$. We furthermore ignore the removed redundant nodes, and use the labelling t_1, t_2, \dots, t_k ; see Note VI.3.

The first step ($j = 1$) is to compute $\text{per } \mathcal{W}_{\circ \alpha^{-1}(1)}$, as depicted in Figure 11a. Here the tree structure $\mathbb{T}_{\circ \alpha^{-1}(1)}$ is almost the same as the initial linear tree of nodes t_1 to t_k , except for the replacement of the root node t_1 by

⁵ We may also choose to walk the tree in the opposite direction. This does not matter.

the dummy root d . Being the first round of the iteration, we need to compute of all the P -tables of the nodes t_k to t_2 (the Q -tables were pre-computed in the preparation phase, see Section VIA 2) and finally $Q[d]$ and $P[d]$ tables of d , whose element $P[d](\rho'(d), \emptyset)$ encodes the value of $\text{per } \mathcal{W}_{\diamond\alpha^{-1}(1)}$.

In step $j = 2$ (Fig. 11b), needed to compute $\text{per } \mathcal{W}_{\diamond\alpha^{-1}(2)}$, the whole subtree T_{t_3} is the same as in the first step and does not need further computation. The only changes to the tree are a new dummy root node d as the parent of t_3 , and the introduction of t_1 as the left child of d , as shown in Figure 11b. This requires only the computation of tables $P[t_1]$ of t_1 and $Q[d]$ and $P[d]$ of d , the last one containing the value of $\text{per } \mathcal{W}_{\diamond\alpha^{-1}(2)}$, found in the entry $P[d](\rho'(d), \emptyset)$.

More generally for step $j > 1$, the head visits the node t_j , replaces it by the dummy d (to compute $\text{per } \mathcal{W}_{\diamond\alpha^{-1}(j)}$), and it furthermore sets d to be the root of the tree by orienting the rest of the tree away. That is, it sets the children of d to be t_{j-1} and t_{j+1} , who are continued by their respective subtrees $T_{t_{j-1}}$ and $T_{t_{j+1}}$. As before, the value $\text{per } \mathcal{W}_{\diamond\alpha^{-1}(j)}$ is contained in $P[d](\rho'(d), \emptyset)$ (where $\rho'(d) = \rho'(t_{j-1}) \cap \rho'(t_{j+1})$; see Note VI.2). To obtain it, it suffices to compute only three tables relating to nodes t_{j-1} and the dummy d , while the rest have been precomputed in previous steps and are reused. This is an important part of our result, summarized below:

Lemma VI.4. *At step $j > 1$ (not initial) of our iterative algorithm described above which computes $\{\text{per } \mathcal{W}_{\diamond\alpha^{-1}(j)}\}_j$ in the order corresponding to tree nodes t_1, t_2, \dots, t_k , the only dynamic programming tables that need to be computed are $P[t_{j-1}]$, $Q[d]$ and $P[d]$.*

Proof. The dummy d is a new node, so we need to compute its tables $Q[d]$ and $P[d]$. We also need to compute $P[t_{j-1}]$ because in the current step j , it has been re-introduced as the parent node of subtree $T_{t_{j-2}}$ and a new child of d . However, no other nodes of the tree have been modified. Specifically, the subtrees $T_{t_{j-2}}$ and $T_{t_{j+1}}$ are the same as in the previous step $j - 1$. This means we can reuse their precomputed tables. Note that Q -tables of nodes never change, and thus they never have to be recomputed. ■

3. Post-processing

Once we have generated an outcome $\underline{r} = (r_1, \dots, r_n)$ of size n , we just need to transform that into a vector of output mode occupations \underline{n}' by counting how many times each outcome mode appears in the vector \underline{r} . Note that the present algorithm assumes that the probability of photon collisions is negligible.⁶ In order to see that this is the

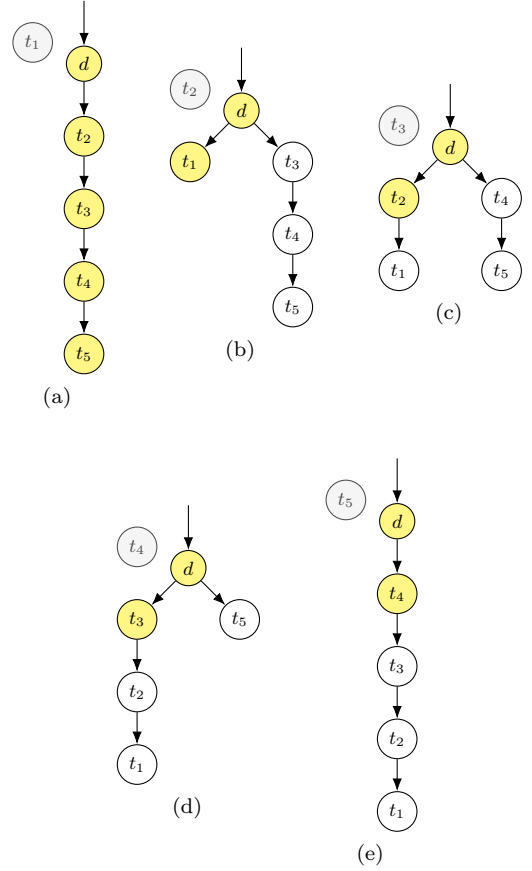


FIG. 11. Computation of $\text{per } \mathcal{W}^{(r_5)}$ using the Laplace expansion: (a) We start with node t_1 corresponding to $\text{per } \mathcal{W}_{\diamond\alpha^{-1}(1)}$. To compute this, replace the node t_1 by a dummy d and run algorithm CP. The P and Q tables of all nodes need to be computed, which is shown by yellow filling. (b) Next, put t_1 back, and replace t_2 by a new dummy d that is now the parent of both t_1 , and of the subtree of t_3 , to compute $\text{per } \mathcal{W}_{\diamond\alpha^{-1}(2)}$. All $Q[t_1], \dots, Q[t_5]$ tables have been computed and remembered in step (a), so we do not recompute them. Observe that each of t_3, \dots, t_5 has the same child (if any) as in step (a), so their P tables do not need to be recomputed either. Marked in yellow are t_1 and d , the only nodes for which we need to compute tables: only $P[t_1]$ for t_1 , and both $Q[d]$ and $P[d]$ for d . (c, d, e) The following steps, corresponding to steps $j = 3, 4, 5$, respectively. In each, we mark yellow the nodes for which we need to compute the dynamic programming tables. At step j , the tables computed are $P[t_{j-1}]$, $Q[d]$ and $P[d]$. The latter contains $\text{per } \mathcal{W}_{\diamond\alpha^{-1}(j)}$ in $P[d](\rho'(d), \emptyset)$. Observe for example in (d) that nodes t_1 and t_2 are not yellow: following the same idea as before, their children (and hence P tables) have not changed from the previous step (c). We conceptualize this as a machine head walking along the tree, at each step replacing the visited node by a dummy and setting it as the root.

⁶ This is because a collision leads to a copied row in $\tilde{\mathcal{V}}^{\underline{r}, \underline{n}}$, or equivalently copies of an output vertex in the corresponding graph $G(\tilde{\mathcal{V}}^{\underline{r}, \underline{n}})$. Generally, this introduces a new cycle, invalidating the tree decomposition of $G(\mathcal{V}^{\underline{n}})$.

correct way to obtain the sample \underline{n}' , we recall the following two facts: A permanent is invariant under permutations of rows, which means only the presence (or more generally, the number of copies) of rows r_i is relevant, and we can

simply count them, obtaining \underline{n}' . Second, recall from Section II C that while the real probability distributions depend on the number basis \underline{n}' , we can indeed use the qudit basis \underline{r} to generate these samples. Indeed, this is one of the insights of Clifford and Clifford [1] that enables generating the sample progressively.

C. Running time asymptotic analysis

In the following, we derive the complexity of our algorithm, looking at the nested loops from the inside out, starting with the Laplace expansion with a k -th marginal with a given r_k . Then we incorporate this into the loop that iterates over all possible values of r_k , and finally the loop over all marginals $k = 2, \dots, n$. Note that the marginals for $k = 1$ are computed separately (line 5) because it is a simple special case; note that its running time is clearly subsumed by the following asymptotics of the more complex marginals.

First, we note that the computation of a Q -table takes time $\mathcal{O}(\omega^2 2^\omega)$ which follows from Lemma C.1. The computation of a P -table of a node with c children takes time $\mathcal{O}(c\omega^2 2^\omega)$ which follows from Lemma C.2. Note both of these lemmas can be found in Appendix C. Both bounds depend on the bound on the size of the contents of the corresponding tree node, which is bounded by the treewidth ω of T^C . Even though we work ubiquitously with restrictions, which may decrease treewidth, we still keep this general bound on the treewidth for simplicity.

To prepare for the Laplace expansion (19b) with a given output r_k , we iterate through the tree as described in the Section VIB 2, computing k permanents. At each step $j = 1, \dots, k$, this requires computing up to three dynamic programming tables $P[t_{j-1}]$, $Q[d]$, and $P[d]$, taking the total time of $\mathcal{O}(\omega^2 2^\omega)$. Recall that the time required to compute P -tables depends on the number of children, which here are known: t_{j-1} has up to one child, and d has up to two. In total, the computation of k permanents takes a total running time of $\mathcal{O}(k2^\omega \omega^2)$.

Sampling r_k takes time $\mathcal{O}(\omega k^2)$, as the Laplace expansion needs k scalar multiplications per possible output, and there are at most $\omega \cdot k$ non-zero outputs. Here, we recall that each column has at most ω rows with nonzero elements, and at this step, we have access to k of those. Note also that this is an upper bound: some columns may be overlapping, in which case the number of possible values of r_k will be lower.

Thus we have shown that the subroutine that computes the k permanents per \mathcal{W}_{\circ_i} runs in time $\mathcal{O}(k2^\omega \omega^2)$ and that computing the marginal probabilities takes extra $\mathcal{O}(k^2 \omega)$ time.

The loop that adds a new photon runs for k in range from 2 to n . Putting this all together, generating a single sample using our algorithm needs the following asymptotic

running time:

$$\sum_{k=1}^n \left(\mathcal{O}(k2^\omega \omega^2) + \mathcal{O}(k^2 \omega) \right) = \mathcal{O}(n^2 2^\omega \omega^2) + \mathcal{O}(\omega n^3).$$

Remark that $\mathcal{O}(\omega n^3)$ remains better than $\mathcal{O}(mn^2)$ while $\omega n < m$. If $\omega n > m$ it is easy to see that by design of our algorithm we recover the scaling $\mathcal{O}(mn^2)$.

For completeness, we shortly note that the preparation (permuting the columns), as well as the restrictions of tree decompositions (which consist of computing set intersections), are subsumed by the above complexity.

VII. CONCLUSION AND FUTURE WORK

We have presented an algorithm that generates samples of n photons from a Boson Sampling experiment on a shallow circuit in the no-collision regime $m = \Omega(n^2)$, a necessary constraint in our algorithm. Combining the central idea of the Boson Sampling simulation work of Clifford and Clifford and the computation of permanent of matrices of with fixed treewidth of Cifuentes and Parrilo, we have constructed an algorithm that generates a sample of n photons from a Boson Sampling experiment in an m -mode circuit described by a matrix of treewidth ω that runs in time $\mathcal{O}(n^2 2^\omega \omega^2) + \mathcal{O}(\omega n^3)$. For the case of shallow circuit, with depth $D = c \log n$, the sampling algorithm becomes polynomial time $\mathcal{O}(n^{2(c+1)} \log^2 n) + \mathcal{O}(n^3 \log n)$, as suggested in [10].

A straightforward use of the Cifuentes and Parrilo result leads to a scaling of $\mathcal{O}(mn^2 2^\omega \omega^2)$ or $\mathcal{O}(n^3 2^\omega \omega^2)$. The former result was attained in [11] by replacing the permanent computations by the algorithm CP, but without optimizing the Laplace expansion on the tree decomposition. Our key technical improvement is to restore the idea of Clifford and Clifford to decouple the dominant running time term from the number of output modes m using the Laplace expansion and precomputing submatrices \mathcal{W}_{\circ_i} in the same running time as needed to compute a permanent of size k . We adapt this idea to the tree decomposition framework of Cifuentes and Parrilo by performing a series of local updates to single nodes that allows us to compute k permanents of subtrees in time comparable to the computation of the permanent of the full tree.

In the regime $\omega = \mathcal{O}(n)$ our sampling algorithm has an extra polynomial cost with respect to the traditional Clifford and Clifford algorithm. An interesting open question would be to find an algorithm that has better scaling than ours and that converges to the exact running time $\mathcal{O}(n2^n)$ when $\omega = n$. Another interesting open problem would be to generalize our result to the collision scenario, where multiple photons can be measured in the same mode. On face value, the latter complicates the use of tree decompositions, because such collisions cause the copying of rows of the matrix whose permanent represents the amplitude, creating a new cycle in its graph. Thus we expect that one would likely need to construct entirely new tree decompositions in such cases.

ACKNOWLEDGMENTS

This work is partially based on work done by S.N. as his 2022 undergraduate final project [22] supervised by R.G.-P., and continued as an LFCS internship over the summer 2022. R.G.-P. was supported by the EPSRC-funded project Benchmarking Quantum Advantage. S.N. thanks William Clements for helpful discussions.

Appendix A: Deferred derivations of section II

1. Boson Sampling outcome probabilities

Here, we fill in the derivation behind equation (12), which follows the steps in [14]. Recall from Section II we have the input (Fock) state $|\underline{n}\rangle \in (\mathbb{C}^n)^{\otimes m}$, corresponding to qudit state

$$|\underline{n}\rangle \cong \frac{1}{\sqrt{n! \cdot \prod_{i=1}^m n_i!}} \sum_{\sigma \in S_n} \sigma |\underline{z}\rangle \in (\mathbb{C}^m)^{\otimes n},$$

where we just used the definition of $|\underline{n}\rangle, |\underline{n}'\rangle$, rearranged the sums over the permutations σ and τ , and decomposed $|\underline{z}\rangle, |\underline{z}'\rangle$ into their individual qudits. Note that the action of the permutations is by braiding, rearranging tensor

where $|\underline{z}\rangle := |1\rangle^{\otimes n_1} \otimes |2\rangle^{\otimes n_2} \otimes \dots \otimes |m\rangle^{\otimes n_m}$ and S_n is the symmetric group on n elements. Analogously, we have the output state $|\underline{n}'\rangle$, which we conventionally represent in qudit space by $|\underline{z}'\rangle$. We denote $|z_j\rangle$ the j^{th} photon (tensor factor) of $|\underline{z}\rangle$, and likewise $|z'_j\rangle$ for $|\underline{z}'\rangle$. Remember that the total number of photons does not change, i.e. $n = \sum_i n_i = \sum_i n'_i = n'$. Recall from the action of \mathcal{U} in the qudit representation (first quantization) in eq. (7):

$$|\underline{z}\rangle = \bigotimes_{k=1}^n |z_k\rangle \xrightarrow{\mathcal{U}^{\otimes n}} \bigotimes_{k=1}^n (\mathcal{U} |z_k\rangle) = \mathcal{U}^{\otimes n} |\underline{z}\rangle.$$

The probability of measuring the output state $|\underline{n}'\rangle$ is given by the Born rule $\mathbb{P}[\underline{n}'|\underline{n}] = |\langle \underline{n}' | \mathcal{U} | \underline{n} \rangle|^2$. We write this in the qudit representation:

$$\begin{aligned} \mathbb{P}[\underline{n}'|\underline{n}] &= \left| \left(\frac{1}{\sqrt{n! \prod_{i=1}^m n_i!}} \sum_{\sigma \in S_n} \langle \underline{z}' | \sigma^{-1} \right) \mathcal{U}^{\otimes n} \left(\frac{1}{\sqrt{n! \prod_{i=1}^m n_i!}} \sum_{\tau \in S_n} \tau |\underline{z}\rangle \right) \right|^2 \\ &= \left| \frac{1}{n! \sqrt{\prod_{i=1}^m n_i! n_i'}} \sum_{\sigma, \tau \in S_n} \left(\bigotimes_{j=1}^n \langle z'_j | \right) \sigma^{-1} \mathcal{U}^{\otimes n} \tau \left(\bigotimes_{k=1}^n |z_k\rangle \right) \right|^2, \end{aligned}$$

factors; this means that the adjoint corresponds to the inverse: $\sigma^\dagger = \sigma^{-1}$, as in $\langle \underline{n}' |$ above.

The permutation σ^{-1} , acting as a braiding of the tensor factors, commutes with the operator $\mathcal{U}^{\otimes n}$, so we can write:

$$\begin{aligned} \mathbb{P}[\underline{n}'|\underline{n}] &= \left| \frac{1}{n! \sqrt{\prod_{i=1}^m n_i! n_i'}} \sum_{\sigma, \tau \in S_n} \left(\bigotimes_{j=1}^n \langle z'_j | \right) \mathcal{U}^{\otimes n} \underbrace{\sigma^{-1} \tau}_{\zeta} \left(\bigotimes_{k=1}^n |z_k\rangle \right) \right|^2 \\ &= \left| \frac{n!}{n! \sqrt{\prod_{i=1}^m n_i! n_i'}} \sum_{\zeta \in S_n} \left(\bigotimes_{j=1}^n \langle z'_j | \right) \mathcal{U}^{\otimes n} \left(\bigotimes_{k=1}^n |z_{\zeta^{-1}(k)}\rangle \right) \right|^2 \end{aligned}$$

where we define the composite $\zeta = \sigma^{-1} \tau$ in S_n . The composite ranges over the whole group S_n , so we remove one summation and get a factor of $n!$ coming from the standard group-theoretic fact that every ζ is a composite of $n!$ different pairs of σ and τ .

Photons in the product $\bigotimes_k |z_k\rangle$ are reordered by ζ : the k -th photon is sent to $\zeta(k)$. We rewrite this state with the

permutation inside. To find which is the k -th factor after the permutation, we apply the inverse ζ^{-1} inside the state to obtain $\bigotimes_k |z_{\zeta^{-1}(k)}\rangle$. Finally, we match up the tensor factors across the expression, giving us terms with $j = k$. This reduces to a product of bra-kets with \mathcal{U} in the middle. To bring the expression into a form of a permanent, we replace the permutation ζ by its inverse $\pi = \zeta^{-1}$. This

reorders the summands, but the summation commutes, so the value is the same. We obtain:

$$\mathbb{P}[\underline{n}'|\underline{n}] = \left| \frac{1}{\sqrt{\prod_{i=1}^m n_i! n_i'}} \sum_{\pi \in S_n} \prod_{j=1}^n \langle z'_j | \mathcal{U} | z_{\pi(j)} \rangle \right|^2$$

This is equation (12) in Section II B, after which the derivation continues in the main text by defining the matrix $\mathcal{V}^{\underline{n}', \underline{n}}$.

Appendix B: Deferred derivations of Section III

1. Marginal probabilities in Algorithm CC-A

In this section, we derive the equation (15) from [1]. Equation (12) gives the probability of outcome $[\underline{n}']$ for an arbitrary input $[\underline{n}]$. We may use the standard input $[\underline{n}] = |1\rangle^{\otimes n} \otimes |0\rangle^{\otimes (m-n)}$, i.e. first n modes are occupied by single photons, and the rest are unoccupied, to omit the reference to $[\underline{n}]$:

$$\mathbb{P}[\underline{n}'] = \frac{|\text{per } \mathcal{V}^{\underline{n}'}|^2}{\prod_{i=1}^m n_i'!}.$$

Recall from section III A the definition of $\tilde{\mathcal{V}}^{(z'_1, \dots, z'_k), \mathcal{C}}$, which fulfils the same function as $\mathcal{V}^{\underline{n}', \underline{n}}$, but it is given by listing which modes appear (qudit representation). The set \mathcal{C} is the set of input modes, i.e. columns of \mathcal{U} , and the output state is represented by $|\underline{z}'\rangle = |z'_1\rangle \otimes \dots \otimes |z'_n\rangle$. We write the probability in this notation, and define the pmf q :

$$q(\underline{z}') := \mathbb{P}[\underline{z}'] = \frac{|\text{per } \tilde{\mathcal{V}}^{(z'_1, \dots, z'_n), [n]}|^2}{\prod_{i=1}^m n_i'!} = \mathbb{P}[\underline{n}']. \quad (\text{B1})$$

By rewriting in terms of qudits, we no longer need to look only at which number state is the output, but also which concrete input photons are in which output mode. We generalize from the non-decreasing states $|z'_1\rangle \dots |z'_n\rangle$ to any ordering of the output photons, represented by the vector $\underline{r} \in [m]^n$. We define a new pmf

$$p(\underline{r}) := \mathbb{P}[\underline{r}] = \frac{|\text{per } \tilde{\mathcal{V}}^{\underline{r}, [n]}|^2}{n!}.$$

The permanent is invariant under permutation of rows and columns, so this is equal to $p(\underline{z}')$, where \underline{z}' are the same modes in non-decreasing order. The number of \underline{r} that correspond to a single \underline{z}' , written $\underline{r} \sim \underline{z}'$, is $\binom{n}{n'_1, \dots, n'_m} = \frac{n!}{\prod_{i=1}^m n_i'!}$. These are distinct ordering of output photons that correspond to the same number state. The two pmfs

are related as:

$$\begin{aligned} \sum_{\underline{r} \sim \underline{z}} p(\underline{r}) &= p(\underline{z}) \sum_{\underline{r} \sim \underline{z}} 1 \\ &= \binom{n}{n'_1, n'_2, \dots, n'_m} \frac{|\text{per } \tilde{\mathcal{V}}^{\underline{z}, [n]}|^2}{n!} \\ &\stackrel{(\text{B1})}{=} \frac{n!}{\prod_{i=1}^m n_i'!} \cdot q(\underline{z}) \end{aligned}$$

Using the qudit representation allows us to work with partial samples of $k < n$ photons, and the definition of $\tilde{\mathcal{V}}^{(z'_1, \dots, z'_k), \mathcal{C}}$ allows us to select which of the incoming photons were measured in the partial sample. The probability of measuring some partial sample $\underline{r}^{(k)} := (r_1, \dots, r_k) \in [m]^k$ of k photons has to sum over the $\binom{n}{k} = \frac{n!}{k!(n-k)!}$ possible subsets of input modes from which these photons came. We arrive at the following:

Lemma B.1 (partial sample). *The marginal pmf of a partial sample of $k \in [n]$ photons is*

$$p(\underline{r}^{(k)}) = \frac{(n-k)!}{n!} \sum_{\substack{\mathcal{C} \subseteq [n] \\ |\mathcal{C}|=k}} |\text{per } \tilde{\mathcal{V}}^{\underline{r}^{(k)}, \mathcal{C}}|^2$$

Proof. To get the marginal pmf, we sum the full pmf over the part of sample \underline{r} that is not in $\underline{r}^{(k)}$, which we call $\underline{r}' = (r_{k+1}, \dots, r_n)$:

$$\begin{aligned} p(\underline{r}^{(k)}) &= \sum_{\underline{r}'} p(\underline{r}) = \sum_{\underline{r}'} \frac{|\text{per } \tilde{\mathcal{V}}^{\underline{r}, [n]}|^2}{n!} \\ &= \frac{1}{n!} \sum_{\underline{r}'} \left(\sum_{\sigma \in S_n} \prod_{j=1}^n \mathcal{U}_{r_j, \sigma_j} \right) \left(\sum_{\tau \in S_n} \prod_{\ell=1}^n \mathcal{U}_{r_\ell, \tau_\ell} \right)^* \end{aligned}$$

where we expanded the definition of permanent, and expressed the magnitude squared $|x|^2 = x x^*$ for any $x \in \mathbb{C}$. Recall that $\tilde{\mathcal{V}}^{\underline{r}, [n]}$ is the matrix with rows r_1, \dots, r_n and columns $[n]$ of \mathcal{U} . Below, we write $\sigma_j \equiv \sigma(j)$, likewise for τ , to shorten the notation.

$$\begin{aligned} p(\underline{r}^{(k)}) &= \frac{1}{n!} \sum_{\underline{r}'} \sum_{\sigma, \tau \in S_n} \prod_{j=1}^n \mathcal{U}_{r_j, \sigma_j} \mathcal{U}_{r_j, \tau_j}^* \quad (\text{B2a}) \\ &= \frac{1}{n!} \sum_{\underline{r}'} \sum_{\sigma, \tau \in S_n} \prod_{j=1}^n \mathcal{U}_{\tau_j, r_j}^\dagger \mathcal{U}_{r_j, \sigma_j} \end{aligned}$$

We have rearranged the expressions. In the right hand side of (B2a), we used the fact that $\mathcal{U}_{r_j, \tau_j}^* = \mathcal{U}_{\tau_j, r_j}^\dagger$. We move the terms not summed over outside of the summation

over $\underline{r}' = (r_{k+1}, \dots, r_n)$:

$$\begin{aligned}
p(\underline{r}^{(k)}) &= \frac{1}{n!} \sum_{\sigma, \tau \in S_n} \left(\prod_{j=1}^k \mathcal{U}_{\tau_j, r_j}^\dagger \mathcal{U}_{r_j, \sigma_j} \right) \sum_{\underline{r}'} \prod_{\ell=k+1}^n \mathcal{U}_{\tau_\ell, r_\ell}^\dagger \mathcal{U}_{r_\ell, \sigma_\ell} \\
&= \frac{1}{n!} \sum_{\sigma, \tau \in S_n} \left(\prod_{j=1}^k \mathcal{U}_{\tau_j, r_j}^\dagger \mathcal{U}_{r_j, \sigma_j} \right) \prod_{\ell=k+1}^n \underbrace{\sum_{r_\ell=1}^m \mathcal{U}_{\tau_\ell, r_\ell}^\dagger \mathcal{U}_{r_\ell, \sigma_\ell}}_{[\mathcal{U}^\dagger \mathcal{U}]_{\tau_\ell, \sigma_\ell}}
\end{aligned} \tag{B2b}$$

In (B2b), we exchange the product and the sum by distributivity. Only one variable (r_ℓ) appears now, but the

product ranges over ℓ , so we still have all the terms. Note that the summation over r_ℓ is a matrix multiplication $\mathcal{U}^\dagger \mathcal{U}$. As \mathcal{U} is unitary, this product is the identity ($\mathcal{U}^\dagger \mathcal{U} = \mathbb{1}$). The product over ℓ then becomes $\prod_{\ell=k+1}^n \delta_{\tau_\ell, \sigma_\ell}$, where $\delta_{i,j}$ is the Kronecker delta. The only nonzero terms are those where $\sigma_\ell = \tau_\ell$ for all $\ell > k$. We partition the permutations as $\sigma = \mu \oplus \zeta$ and $\tau = \nu \oplus \zeta$ into a shared part $\zeta \in S_{n-k}$ (this is the part that ensures $\sigma_\ell = \tau_\ell$ for $\ell > k$), and $\mu, \nu \in S_k$, which may be different. This means we also partition the set $[n]$ on which σ, τ act into a subset \mathcal{C} of size k on which μ, ν act, and $[n] \setminus \mathcal{C}$ acted upon by ζ .⁷ We rewrite the summation over σ and τ as summations over the selection of $\mathcal{C} \subseteq [n]$, i.e. over the partitions, such that we select the part of $[n]$ where μ, ν act, and as summations over μ, ν themselves. For each \mathcal{C} , there are $(n-k)!$ possible permutations ζ ; this gives the new factor in (B2c):

$$p(\underline{r}^{(k)}) = \frac{(n-k)!}{n!} \sum_{\mathcal{C} \subseteq [n]; |\mathcal{C}|=k} \underbrace{\left(\sum_{\mu \in S_{\mathcal{C}}} \prod_{j=1}^k \mathcal{U}_{r_j, \mu_j} \right)}_{\text{per } \tilde{\mathcal{V}}^{\mathcal{C}, (r_1, \dots, r_k)}} \underbrace{\left(\sum_{\nu \in S_{\mathcal{C}}} \prod_{\ell=1}^k \mathcal{U}_{r_\ell, \nu_\ell} \right)^*}_{(\text{per } \tilde{\mathcal{V}}^{\mathcal{C}, (r_1, \dots, r_k)})^*} \tag{B2c}$$

$$= \frac{(n-k)!}{n!} \sum_{\mathcal{C} \subseteq [n]; |\mathcal{C}|=k} \left| \text{per } \tilde{\mathcal{V}}^{\underline{r}^{(k)}, \mathcal{C}} \right|^2 \tag{B2d}$$

Thus we have recovered the permanent of submatrices, and this concludes the proof. ■

The algorithms of CC expand the sample size (number of photons) progressively. This is an application of the chain rule for probability: $\mathbb{P}[A, B] = \mathbb{P}[A|B] \cdot \mathbb{P}[B]$, which in our case gives

$$\begin{aligned}
p(\underline{r}) &= p(r_n | r_1, \dots, r_{n-1}) \cdot p(r_1, \dots, r_{n-1}) \\
&= p(r_n | r_1, \dots, r_{n-1}) \cdot p(r_{n-1} | r_1, \dots, r_{n-2}) \cdots p(r_1),
\end{aligned}$$

or written in terms of expanding the sample to $k+1$ photons:

$$p(\underline{r}^{(k+1)}) = p(r_{k+1} | \underline{r}^{(k)}) \cdot p(\underline{r}^{(k)}).$$

The Clifford and Clifford algorithms compute the $p(r_{k+1} | \underline{r}^{(k)})$.

2. Marginal probabilities in Algorithm CC-B

In the previous Section B1, we derived the marginal probability of a partial sample $\underline{r}^{(k)}$ of k photons in equation (B2d). There, we have to sum over the subsets

$\mathcal{C} \subseteq [n]$ of size k to select which k input photons are those that we measured in $\underline{r}^{(k)}$.

In [1], going from CC-A to CC-B, the idea is to remove that selection from the marginal itself, and instead determine the order in which input photons appear. This order is chosen randomly for each full sample. This means each sample comes from a simpler probability distribution, but the ensemble of many samples follows the correct distribution.

As part of the initialization of the algorithm, i.e. before the sample is generated, choose a uniformly random permutation $\alpha \in S_n$. At each k , the set \mathcal{C} will be defined to be $\mathcal{C} = \alpha([k]) = \{\alpha(1), \dots, \alpha(k)\}$. For each \mathcal{C} of size k , there are $k!(n-k)!$ permutations α such that $\mathcal{C} = \alpha([k])$, so we need to divide by this to preserve equality:

$$\begin{aligned}
p(\underline{r}^{(k)}) &= \frac{1}{n! k!} \sum_{\alpha \in S_n} \left| \text{per } \tilde{\mathcal{V}}^{\underline{r}^{(k)}, \alpha([k])} \right|^2 \\
&= \mathbb{E}_{\alpha \in S_n} \underbrace{\left[\frac{1}{k!} \left| \text{per } \tilde{\mathcal{V}}^{\underline{r}^{(k)}, \alpha([k])} \right|^2 \right]}_{\phi(\underline{r}^{(k)} | \alpha)},
\end{aligned}$$

which is equation (17) in the main text (Section III B). We see that the original pmf p is the expectation of a different pmf called ϕ , taken over the uniformly random $\alpha \in S_n$, where ϕ is conditioned on α .

⁷ For consistency, use the notation \mathcal{C} for this set because these are indeed the sets of columns in our tree decompositions.

Appendix C: Deferred derivations of Section IV

1. Running time details

In this section, we derive the running time of algorithm CP. See [2, Theorem 12, Lemma 2].

In the following, we have a matrix $M \in \mathbb{C}^{n \times n}$, a tree decomposition $T = (T, \rho, \kappa)$ of its graph $G(M)$, and this tree decomposition has treewidth ω .

Lemma C.1. *For a node $t \in T$, computing the table $Q[t]$ takes time $\mathcal{O}(\omega^2 2^\omega)$.*

Proof. (See Lemma 2 in [2].) We compute the table $Q[t]$ for pairs of subsets $R \subseteq \rho(t)$ and $C \subseteq \kappa(t)$, with values $Q[t](R, C) = \text{per}_M(R, C)$ by Laplace expansion:

$$\text{per}_M(R, C) = \sum_{c \in C} M_{r,c} \text{per}_M(R \setminus r, C \setminus c),$$

where $r \in R$ is a selected row (we choose it to be $r = \min R$ for convenience). Note that $\text{per}_M(\emptyset, \emptyset) = 1$ and $\text{per}_M(R, C) = 0$ if the sizes do not match, i.e. $|R| \neq |C|$. Thus we only need to compute permanents of square submatrices selected from the node t . We do this by starting with the 1×1 matrices, and then increase size, on each step using the Laplace expansion.

There are $\mathcal{O}(2^{|\rho(t)|+|\kappa(t)|}) = \mathcal{O}(2^\omega)$ values to compute: this is the size of the domain, though this is an upper bound, because as mentioned above, some of the entries are always zero. We note that ω is the treewidth, so for any node $t \in T$, the size of its contents is $|\rho(t)| + |\kappa(t)| - 1 \leq \omega$. For each of those steps, we need $\mathcal{O}(|\kappa(t)|) = \mathcal{O}(\omega)$ operations – this is the number of columns in the summation. Finally, for each summand, we need $\mathcal{O}(\omega)$ time to find the sets $R \setminus r, C \setminus c$ and look up the stored value of the corresponding permanent. Thus, the time is bounded as $\mathcal{O}(\omega^2 2^\omega)$. ■

Lemma C.2. *For an internal node $t \in T$, computing the table $P[t]$ takes time $\mathcal{O}(k_t \omega^2 2^\omega)$, where k_t is the number of children of t .*

Proof. (See Theorem 12 in [2].) First note that the helper tables $Q'[t|c_j]$ and $Q''[t \leftarrow c_j]$ for each child c_j of t do not require any computation: they simply reference $Q[t]$ and $P[c_j]$ (in the latter case with a change in argument). The actual computation happens in the subset convolution, which is done in time $\mathcal{O}(k_t \omega^2 2^\omega)$, where Cifuentes & Parrilo adapt the method from [23]. ■

Theorem C.3 (running time of CP). *We can compute per M in time $\mathcal{O}(n 2^\omega \omega^2)$.*

Proof. (See Theorem 15, and also Theorem 5 for more context, in [2].) To compute the permanent from the whole tree, we have to compute the tables $Q[t]$ and then $P[t]$ for all $t \in T$, which takes the times obtained from Lemmas C.1 and C.2 for each node.

This gives $\mathcal{O}(|T| \omega^2 2^\omega)$ for the Q tables. We bound $|T| = \mathcal{O}(n)$, i.e. the size of the tree is linear in the number of columns (and rows) of the matrix. This is an assumption that we choose a reasonable tree decomposition: we could have a much larger tree, but at that point it would contain a lot of redundancy. Note that in every tree decomposition used in this paper, it is indeed the case that $|T| = \mathcal{O}(n)$.

For the P tables, we also note the following: $\sum_{t \in T} k_t = |T| - 1$, i.e. summing the numbers of all children gives the number of non-root nodes: this is because the root is not a child. Then

$$\begin{aligned} \sum_{t \in T} \mathcal{O}(k_t \omega^2 2^\omega) &= \mathcal{O}(\omega^2 2^\omega \sum_{t \in T} k_t) \\ &= \mathcal{O}(|T| \omega^2 2^\omega) \\ &= \mathcal{O}(n \omega^2 2^\omega). \end{aligned}$$

Thus we have the bound on the time taken to compute all Q and P tables, and hence the permanent. ■

Appendix D: Deferred derivations of Section V

1. Restriction of tree decomposition corresponds to submatrix

Proof of Lemma V.8. We have a tree decomposition $T = (T, \rho, \kappa)$ of $G(\mathcal{U})$, the graph of matrix \mathcal{U} . Let $\mathcal{R}' \subseteq \mathcal{R}$ be a subset of rows, and $\mathcal{C}' \subseteq \mathcal{C}$ of columns. These define a submatrix $\mathcal{U}' := \mathcal{U}|_{\mathcal{R}', \mathcal{C}'}$ of \mathcal{U} with rows \mathcal{R}' and columns \mathcal{C}' , and we want to show that a restriction $T|_{\mathcal{R}', \mathcal{C}'} = (T, \rho', \kappa')$ of the decomposition T to those subsets is a tree decomposition of the graph $G(\mathcal{U}')$. Recall that both T and $T|_{\mathcal{R}', \mathcal{C}'}$ have the same tree T , but the contents of nodes in $T|_{\mathcal{R}', \mathcal{C}'}$ are defined as $\rho'(t) = \rho(t) \cap \mathcal{R}'$ and $\kappa'(t) = \kappa(t) \cap \mathcal{C}'$ for all $t \in T$.

First, check (T1), i.e. the Axiom requiring that all vertices are included in the tree decomposition:

$$\bigcup_{t \in T} \rho'(t) = \bigcup_{t \in T} [\rho(t) \cap \mathcal{R}'] = \left[\bigcup_{t \in T} \rho(t) \right] \cap \mathcal{R}' \quad (\text{D1a})$$

$$\stackrel{(\text{T1})}{=} \mathcal{R} \cap \mathcal{R}' \stackrel{(\mathcal{R}' \subseteq \mathcal{R})}{=} \mathcal{R}'. \quad (\text{D1b})$$

We omit the analogous steps to show $\bigcup_t \kappa'(t) = \mathcal{C}'$. Thus, we conclude that $T|_{\mathcal{R}', \mathcal{C}'}$ satisfies Axiom (T1) with respect to $G(\mathcal{U}')$.

Now, we show that $T|_{\mathcal{R}', \mathcal{C}'}$ satisfies (T2) w.r.t. the graph $G(\mathcal{U}')$ of the submatrix. Note that $G(\mathcal{U}')$ is an induced subgraph of $G(\mathcal{U})$, meaning that for each edge $(|i\rangle, \langle j|)$ in $G(\mathcal{U})$, if its endpoints are in $G(\mathcal{U}')$, then the edge is in $G(\mathcal{U}')$ as well (with the same weight). By (T2) on T w.r.t. $G(\mathcal{U})$, for every edge $(|i\rangle, \langle j|)$, there is a node $t \in T$ containing it, i.e. $|i\rangle \in \rho(t)$ and $\langle j| \in \kappa(t)$. If $|i\rangle \in \mathcal{R}'$ and $\langle j| \in \mathcal{C}'$, then by definition of the restriction

they belong to $\rho'(t)$ and $\kappa'(t)$. Hence (T2) holds for $T|_{\mathcal{R}',\mathcal{C}'}$ with respect to $G(\mathcal{U}')$.

We finish by showing that (T3) holds for $T|_{\mathcal{R}',\mathcal{C}'}$ w.r.t. $G(\mathcal{U}')$. Define the preimage of ρ as $\rho^{-1} : \mathcal{R} \rightarrow 2^T$ where $\rho^{-1}(|i\rangle) = \{t \in T \mid |i\rangle \in \rho(t)\}$ for all $|i\rangle \in \mathcal{R}$. Define the preimage κ^{-1} analogously. These give us the set of nodes that contain a row or column. By Axiom (T3) that holds for T w.r.t. $G(\mathcal{U})$, each $\rho^{-1}(|i\rangle)$ (resp. $\kappa^{-1}(|j\rangle)$) forms a subtree of T . Under the restriction to \mathcal{R}' and \mathcal{C}' , the preimages are clearly $(\rho')^{-1} = \rho^{-1}|_{\mathcal{R}'}$ and $(\kappa')^{-1} = \kappa^{-1}|_{\mathcal{C}'}$. Thus for any row $|i\rangle \in \mathcal{R}'$ (resp. column $|j\rangle \in \mathcal{C}'$), the set of nodes containing it $(\rho')^{-1}(|i\rangle)$ (resp. $(\kappa')^{-1}(|j\rangle)$) is a subtree of T , and the Axiom (T3) is satisfied for $T|_{\mathcal{R}',\mathcal{C}'}$ as a tree decomposition of $G(\mathcal{U}')$.

We conclude that the restriction $T|_{\mathcal{R}',\mathcal{C}'}$ is a valid tree decomposition, and that is it the decomposition of $G(\mathcal{U}')$, the graph of the submatrix $\mathcal{U}' = \mathcal{U}|_{\mathcal{R}',\mathcal{C}'}$. ■

2. Redundancy of nodes

Proof of Lemma V.10. We verify that $T \setminus t$ satisfies the Axioms from Definition IV.1 with respect to the graph $G(M)$ of M . Recall that $G(M)$ has vertices $\mathcal{R} \sqcup \mathcal{C}$, where \mathcal{R} is the set of row labels and \mathcal{C} of column labels. There is an edge $(|i\rangle, |j\rangle)$ iff M_{ij} is nonzero.

In the original tree decomposition T , by Axiom (T1), $\rho(T) = \bigcup_{q \in T} \rho(q) = \mathcal{R}$ and similarly $\kappa(T) = \mathcal{C}$. In our case, node t has no columns ($\kappa(t) = \emptyset$), so $\kappa(T \setminus t) = \mathcal{C}$ already. Removing t does not violate Axiom (T1) on columns.

We verify the same for rows: We have $\rho(T) = \mathcal{R}$ and $\rho(t) \subseteq \rho(T \setminus t)$. This implies that

$$\mathcal{R} = \rho(T) = \rho(t) \cup \rho(T \setminus t) = \rho(T \setminus t).$$

Thus $T \setminus t$ satisfies Axiom (T1).

Now, verify Axiom (T2), stating that every edge must be contained in a node. The decomposition T satisfies this. Node t has $\kappa(t) = \emptyset$, so it cannot contain any edges. Therefore all edges are contained in $T \setminus t$, and thus the latter satisfies Axiom (T2).

Finally, we verify Axiom (T3) stating that the set of all nodes containing a row (resp. column) forms a subtree of T . We reuse notation from Sec. D 1, where $\rho^{-1}(|i\rangle)$ is the set of all nodes containing $|i\rangle$, and analogously for κ^{-1} . We split the tree into subtrees T_1 of all ancestors of t , and T_2 of all descendants of t , both excluding t itself.

For any column $|j\rangle \in \mathcal{C}$, $\kappa^{-1}(|j\rangle)$ is contained either in T_1 or T_2 . This is because $\kappa^{-1}(|j\rangle)$ must be a subtree, and thus connected. However, T_1 and T_2 are only connected through t which contains no columns, so $t \notin \kappa^{-1}(|j\rangle)$.

The situation is more complicated with rows, because we do not exclude them from t . Define $R_1 = \rho(T_1) \setminus \rho(T_2)$, similarly $R_2 = \rho(T_2) \setminus \rho(T_1)$, that is sets of rows contained in one subtree, but not the other. Note that there may be rows contained in both: define $R_\cap = \rho(T_1) \cap \rho(T_2)$. By Axiom (T3), the rows in R_\cap are contained in t . We require that $\rho(t) \subseteq \rho(T \setminus t)$, so t cannot contain any other rows. In $T \setminus t$, where we delete node t and connect T_1 to T_2 directly, Axiom (T3) still holds: this is trivial for rows in R_1 and R_2 . For $|i\rangle \in R_\cap$, its subtree $\rho^{-1}(|i\rangle)$ in T is a subtree of T with nodes from T_1 , T_2 , and including t . By deleting t and connecting T_1 to T_2 , we ensure that $\rho^{-1}(|i\rangle)$ is a subtree of $T \setminus t$. We conclude that (T3) holds for $T \setminus t$. ■

Example D.1 (disjoint graphs). As an illustrative special case, suppose that t has no columns as above, and also no rows, i.e. $\rho(t) = \emptyset$. This clearly satisfies the conditions of Lemma V.10. Denote T_1 the set of ancestors of t and T_2 the set of descendants of t , both subtrees of T . Since t is completely empty, by Axiom (T3), the two trees T_1 and T_2 correspond to blocks of the matrix which share no rows nor columns. We can also view this as joining together two independent graphs (and their tree decompositions), by putting an empty node between them. Up to an appropriate permutation of rows and columns, corresponding to a change of basis, the matrix is block diagonal and its permanent is the product of permanents of blocks. In terms of the tree decomposition, the value $P[t](\emptyset, \emptyset)$ (which is the only entry in the table $P[t]$) stores the permanent of the tree T_2 .

Note D.2. An important formal detail is that $T \setminus t$ is not equivalent (for computing the permanent) to T if there exists a row vertex $|i\rangle \in \rho(t)$ that is not contained in any other node, i.e. when the requirement that $\rho(t) \subseteq \rho(T \setminus t)$ is violated. Since $\kappa(t) = \emptyset$, there is no column vertex to which $|i\rangle$ could be connected, and this corresponds to having a row of all zeros in the matrix. So far, we assumed this cannot be the case. However, we have to be careful about this when taking restrictions: Suppose there is a column $|j\rangle$ that has a single non-zero value in row $|i\rangle$. A restriction that removes $|j\rangle$ must also remove $|i\rangle$ (and any other similar rows); otherwise, the decomposition would no longer represent the matrix correctly.

[1] P. Clifford and R. Clifford, The classical complexity of boson sampling, in *SODA* (2018).
[2] D. Cifuentes and P. A. Parrilo, An efficient tree decomposition method for permanents and mixed discriminants, *Linear Algebra and its Applications* **493**, 45 (2016).
[3] S. Aaronson and A. Arkhipov, The computational com-

plexity of linear optics, *Theory of Computing* **9**, 143 (2013).
[4] J. Preskill, *Quantum computing and the entanglement frontier* (2012).
[5] L. Valiant, The complexity of computing the permanent, *Theoretical Computer Science* **8**, 189 (1979).

- [6] H. J. Ryser, *Combinatorial mathematics*, The Carus Mathematical Monographs, Vol. No. 14 (Mathematical Association of America, ; distributed by John Wiley and Sons, Inc., New York, 1963) pp. xiv+154.
- [7] D. G. Glynn, The permanent of a square matrix, *European Journal of Combinatorics* **31**, 1887 (2010).
- [8] H.-S. Zhong, H. Wang, Y.-H. Deng, M.-C. Chen, L.-C. Peng, Y.-H. Luo, J. Qin, D. Wu, X. Ding, Y. Hu, P. Hu, X.-Y. Yang, W.-J. Zhang, H. Li, Y. Li, X. Jiang, L. Gan, G. Yang, L. You, Z. Wang, L. Li, N.-L. Liu, C.-Y. Lu, and J.-W. Pan, Quantum computational advantage using photons, *Science* **370**, 1460 (2020), <https://www.science.org/doi/pdf/10.1126/science.abe8770>.
- [9] H.-S. Zhong, Y.-H. Deng, J. Qin, H. Wang, M.-C. Chen, L.-C. Peng, Y.-H. Luo, D. Wu, S.-Q. Gong, H. Su, Y. Hu, P. Hu, X.-Y. Yang, W.-J. Zhang, H. Li, Y. Li, X. Jiang, L. Gan, G. Yang, L. You, Z. Wang, L. Li, N.-L. Liu, J. J. Renema, C.-Y. Lu, and J.-W. Pan, Phase-programmable gaussian boson sampling using stimulated squeezed light, *Phys. Rev. Lett.* **127**, 180502 (2021).
- [10] R. García-Patrón, J. J. Renema, and V. Shchesnovich, Simulating boson sampling in lossy architectures, *Quantum* **3**, 169 (2019).
- [11] C. Oh, Y. Lim, B. Fefferman, and L. Jiang, *Classical simulation of boson sampling based on graph structure* (2021).
- [12] H. Qi, D. Cifuentes, K. Brádler, R. Israel, T. Kala-jdziewski, and N. Quesada, Efficient sampling from shallow gaussian quantum-optical circuits with local interactions (2020), [arXiv:2009.11824 \[quant-ph\]](https://arxiv.org/abs/2009.11824).
- [13] P. Kok and B. W. Lovett, *Introduction to Optical Quantum Information Processing* (Cambridge University Press, 2010).
- [14] A. E. Moylett and P. S. Turner, Quantum simulation of partially distinguishable boson sampling, *Phys. Rev. A* **97**, 062329 (2018).
- [15] A. J. Walker, New fast method for generating discrete random numbers with arbitrary frequency distributions, *Electronics Letters* **10**, 127 (1974).
- [16] G. Voigt, *Tree decompositions, treewidth, and NP-hard problems* (2016).
- [17] J. Carolan, C. Harrold, C. Sparrow, E. Martín-López, N. J. Russell, J. W. Silverstone, P. J. Shadbolt, N. Matsuda, M. Oguma, M. Itoh, G. D. Marshall, M. G. Thompson, J. C. F. Matthews, T. Hashimoto, J. L. O'Brien, and A. Laing, Universal linear optics, *Science* **349**, 711 (2015), <https://www.science.org/doi/pdf/10.1126/science.aab3642>.
- [18] B. A. Bell and I. A. Walmsley, Further compactifying linear optical unitaries, *APL Photonics* **6**, 070804 (2021), <https://doi.org/10.1063/5.0053421>.
- [19] R. Jozsa, On the simulation of quantum circuits, *arXiv: Quantum Physics* (2006).
- [20] R. A. Campos, B. E. A. Saleh, and M. C. Teich, Quantum-mechanical lossless beam splitter: SU(2) symmetry and photon statistics, *Phys. Rev. A* **40**, 1371 (1989).
- [21] W. R. Clements, P. C. Humphreys, B. J. Metcalf, W. S. Kolthammer, and I. A. Walmsley, Optimal design for universal multiport interferometers, *Optica* **3**, 1460 (2016).
- [22] S. Novák, Efficient simulation of shallow quantum circuits: Boson Sampling (2022), bachelor's dissertation, University of Edinburgh.
- [23] A. Björklund, T. Husfeldt, P. Kaski, and M. Koivisto, Fourier meets Möbius: Fast subset convolution, in *Proceedings of the Thirty-Ninth Annual ACM Symposium on Theory of Computing*, STOC '07 (Association for Computing Machinery, New York, NY, USA, 2007) p. 67–74.